TWO-STAGE RECEIVER STRUCTURES FOR CONVOLUTIONALLY-ENCODED DS-CDMA SYSTEMS *

Ayman Y. Elezabi Alexandra Duel-Hallen
Electrical and Computer Engineering Department
Box 7911
North Carolina State University
Raleigh, NC 27695-7911
aelezabi@yahoo.com, sasha@eos.ncsu.edu

Abstract

We consider alternative structures for subtractive interference cancellation (IC) detectors with single-user Viterbi decoding for convolutionally encoded code-division multiple-access (CDMA) systems on synchronous additive white Gaussian noise (AWGN) and time-uncorrelated Rayleigh fading channels. In the first structure interference cancellation with undecoded decisions (ICUD) is performed followed by single-user decoding of each user. In the second structure post-decoding interference cancellation (PDIC) is applied followed by a second bank of single-user decoders. As expected, the PDIC scheme usually outperforms the ICUD but we find some special cases where the performance of the ICUD is better. This behavior is analyzed and conditions for the existence of an error probability floor for ICUD receivers are derived. Furthermore, a multiuser interleaving scheme, in which each user is assigned a distinct interleaving pattern (DIP), is proposed for the PDIC scheme to overcome a problem caused by decoding prior to IC. The performance gain due to DIP is significant on the AWGN channel and, for a small number of users, on the time-uncorrelated fading channel. By analyzing the residual multiple-access interference (RMAI), we project that the performance gain due to DIP will be significant on time-correlated channels with slow fading even for a large number of users. The complexity of the proposed DIP scheme is analyzed and its applicability to the asynchronous AWGN channel and multipath fading environments is discussed. Finally, a family of approximations to the bit error rate (BER) and some exact results are derived for the various receiver structures. In particular, a novel expression for the variance of the RMAI in the ICUD receiver is derived and shown to improve the accuracy of the BER approximation. CDMA systems using both deterministic and random spreading sequences are considered.

*This research was supported by NSF grants CCR-9725271 and CCR-981-5002 and ARO grant DAA-19-01-1-0638

1 Introduction

The performance of code-division multiple-access (CDMA) systems is mainly limited by multiple-access interference (MAI) in addition to the fading encountered on the mobile radio channel where CDMA systems are typically used. Mitigating MAI, therefore, leads to systems with higher capacity. The simplest receiver to implement is the so-called "conventional" or matched filter receiver which, for any given user, consists of a filter matched to the spreading (signature) sequence of that user, followed by a threshold decision device. Because it does not utilize the knowledge of interfering users' parameters, the performance of the conventional receiver is generally poor. On the other hand, the maximum-likelihood multi-user detector [1] is near-optimal in terms of error probability but has complexity that is exponential in the number of users, rendering it impractical for most applications. This has resulted in a huge effort in search of multiuser detectors with reasonable complexity that overcome the shortcomings of the conventional receiver. Multi-stage, or subtractive IC, detectors [2] are a large family of detectors that offer attractive trade-offs between performance, complexity, and demodulation delay. In this class of detectors, a first stage produces tentative decisions or estimates for all the users' bits which are then used in subsequent stages to subtract MAI from the signals of each user. These detectors can be easily combined with single-user decoders to improve the interference cancellation (IC) operation itself, which is very important since virtually all practical systems employ some form of forward error correction.

The maximum-likelihood joint multiuser detector and decoder for asynchronous convolutionally encoded CDMA systems [3] has complexity that is exponential in the product of the number of users and the constraint length of the encoder. Furthermore, suboptimal implementations of the ML joint detector and decoder, such as reduced-state sequence estimation or sequential decoding approaches (see references in [4, p.1192-1193]), are still too complex. On the other hand, complete partitioning of the multiuser detection and decoding functionality in the receiver is undesirable since it does not make use of the coding on the link to improve the interference cancellation (IC) and thus it limits performance considerably for highly loaded systems. We refer to this type of receiver as an IC with Undecoded Decisions (ICUD) detector. One practical solution to the problem is possible with subtractive IC detectors where single-user Viterbi decoders (VDs) may be employed prior to the IC stage to produce better first stage decisions and thus more reliable MAI cancellation. We call this receiver structure Post-Decoding IC (PDIC). While more complex than ICUD, this approach utilizes the coding on the link in the IC stage(s) and avoids the complexity of joint ML-based detectors and decoders. This approach was suggested in [5] for a code-spread CDMA system using successive IC and was considered among other proposals in [4].

In this paper we focus on parallel-IC two-stage receivers with the conventional first stage making hard decisions and single-user soft-decision VDs with hard outputs. We limit ourselves to only one

stage of IC following the conventional first stage for acceptable hardware complexity and demodulation delay. The proposed receiver structures, however, can be easily extended to additional IC stages. We compare the PDIC and ICUD receivers under various conditions and identify interesting special cases when the ICUD receiver outperforms the PDIC receiver. This prompts an examination of the residual MAI (RMAI) in both structures. Analytical results concerning the existence of error probability floor for ICUD receivers are derived. We also find that the decoding in PDIC schemes causes the RMAI to be correlated in such a way that requires special interleaving among the users. To our knowledge, little attention has been given in the literature to the interleaving problem in PDIC structures. In [6] a successive IC scheme is proposed with random interleaving that reduces the demodulation delay but no connection is made between the statistics of the RMAI terms and the interleaving properties. In this paper we propose a multiuser interleaving scheme that improves the performance of the PDIC receiver by assigning each user a distinct interleaving pattern (DIP). We analyze the factors that affect the performance gain due to DIP and demonstrate this gain under different conditions using computer simulations. We also obtain approximations and some exact results for the BER of the receiver structures considered. In approximating the BER of ICUD receivers, the dependence between the variables comprising the RMAI terms precludes straightforward computation of the variance of the total RMAI. By taking into account the strong dependence between some of the variables and ignoring the weak dependence among the remaining ones, we derive a novel estimate of the variance of the RMAI terms that results in a more accurate application of the standard Gaussian approximation.

In our simulations and performance analysis we consider synchronous channel models for both the AWGN and frequency-nonselective time-uncorrelated Rayleigh fading channel although a discussion of the asynchronous and multipath fading channels is also included. The synchronous model represents a worst-case scenario in terms of interference [7] and for large systems can be approximated by an asynchronous system with twice the number of users. Hence, the synchronous model does not limit our qualitative conclusions about the relative performance of the different receiver structures. The time-uncorrelated fading model reflects rapidly time-variant channels with sufficient interleaving depth. However, time-correlated fading channels result in worse RMAI and hence the improvement due to DIP is expected to be larger. We consider systems with both deterministic, i.e. short, and random, i.e. long, spreading sequences. The BER expressions are slightly different for both types and so are the conclusions concerning the performance gain due to DIP.

The organization of the paper is as follows. In section 2, the system model is explained and assumptions stated. The two IC schemes, ICUD and PDIC, are described and compared and conclusions are drawn about the relative performance of both structures under various conditions. Two analytical results concerning the BER floor of the ICUD structure are given and their implications discussed. In section 3 the need for a special interleaving scheme for PDIC structures, where each

user is assigned a DIP, is explained. An example DIP scheme is proposed and shown to accommodate a large number of users. Asynchronous multipath channels are discussed and an analysis of the implementation complexity is included. In section 4, performance comparisons are given between the PDIC scheme, with and without DIP, and the ICUD scheme for both the AWGN and frequency-nonselective flat Rayleigh fading channel. section 5 describes an approximate method for obtaining the BER for both PDIC and ICUD structures. Exact expressions for the BER of the conventional first stage and the pairwise error probability at the output of the conventional first stage are derived. A novel estimate of the variance of RMAI after IC is also given for single-path Rayleigh fading channels and derived in the appendix and the improvement in approximating the BER is demonstrated. The applicability of the standard Gaussian approximation for IC receivers is also discussed. Finally, a discussion of some practical issues and concluding remarks are given in section 6.

2 Alternative IC Structures and Relative Performance

Consider K users transmitting synchronously using binary CDMA signaling over a frequency-nonselective Rayleigh fading channel. At the receiver, a bank of K matched filter correlators despreads each user's signal as shown in Figure 1, where the signature sequence of user k is given by s_k. Sampling at the bit rate, we can write the output of the correlator bank for a given sample point at baseband as

$$y_k(1) = c_k b_k + \sum_{j=1, j\neq k}^{K} r_{kj} c_j b_j + n_k \qquad k = 1, \ldots, K \tag{1}$$

where the argument in the parentheses denotes the stage number, $c_k = |c_k| e^{\jmath\theta_k}$ are independent zero-mean complex Gaussian fading coefficients, $b_k \in \{-1, +1\}$ is the data bit of user k, n_k is a zero-mean complex Gaussian additive noise term with variance $\sigma^2 = \frac{1}{2}\mathbf{E}[n_k^* \, n_k]$, and r_{kj} is the normalized crosscorrelation between the signature sequences of users k and j. The covariance between the real as well as between the imaginary parts of n_j and n_k is equal to $r_{kj}\sigma^2$. The signal-to-noise ratio (SNR) for user j is defined as $\gamma_j = \frac{1}{2}\frac{\mathbf{E}[|c_j|^2]}{\sigma^2}$. We consider the interleaver size to be sufficient to render the fading coefficients uncorrelated from one bit interval, or sample point, to another. This model represents high-mobility applications where the coherence time is sufficiently short. We shall also discuss slowly fading channels in section 3 on multiuser interleaving and in section 6, the Conclusions. For coherent reception, the conventional first stage decision about the bit of user k is given by $\hat{b}_k(1) = \mathrm{sgn}[\grave{y}_k(1)]$ where

$$\grave{y}_k(1) = \mathbf{Re}[e^{-\jmath\theta_k} y_k(1)] = |c_k| b_k + \sum_{j=1, j\neq k}^{K} r_{kj} |c_j| \beta_{jk} b_j + \grave{n}_k \tag{2}$$

where $\beta_{jk} = \cos(\theta_j - \theta_k)$, and $\{\grave{n}_j\}$ have the same joint distribution as $\{\mathbf{Re}(n_j)\}$ or $\{\mathbf{Im}(n_j)\}$. The output of the second stage, i.e. after one stage of Interference Cancellation (IC), for user 1 (henceforth, our user of interest) is given by

$$\grave{y}_1(2) = |c_1|b_1 + \sum_{j=2}^{K} 2r_{1j}|c_j|\beta_{j1}e_j + \grave{n}_1 \stackrel{\triangle}{=} |c_1|b_1 + \zeta + \grave{n}_1 \tag{3}$$

where $e_j = \frac{1}{2}(b_j - \hat{b}_j(1))$ represents the error in the first stage decision of user j and $\zeta \stackrel{\triangle}{=} \sum_j \zeta_j$ is the total RMAI, where ζ_j is the RMAI due to user j. For the uncoded system, the final decisions are given by $\hat{b}_k(2) = \mathrm{sgn}[\grave{y}_k(2)]$, whereas for a system with channel coding, a bank of single-user soft decision VDs operates on $\{\grave{y}_k(2)\}$ to produce the final decisions. Throughout the paper, we assume that perfect channel estimates are available at the receiver for the IC stages and soft-decision VDs. While two-stage detectors (TSDs) may be quite sensitive to channel mismatch [8], practical systems employing pilot symbols or a pilot channel, e.g. [9], can result in near perfect channel estimation. Hence, we do not further address the issue of imperfect channel estimates in our work. The sensitivity of parallel IC detectors to phase and timing errors, while not an issue for our phase-synchronous model, has been studied in [10] and it was concluded that the parallel IC was fairly robust to phase and timing errors. This conclusion should carry over naturally to IC receivers which include decoders for convolutionally coded CDMA systems. In addition to the fading channel model described above, we study the synchronous unfaded AWGN channel via computer simulations, in which case c_k in (1) represents the fixed (real) amplitude of the signal and $\{n_k\}$ are real-valued in the above equations. In addition to the importance of the AWGN channel model in its own right, our conclusions for the relative performance of the two receiver structures, ICUD and PDIC, and the DIP scheme are different for both the AWGN and fading channels. The applicability of the proposed receiver structures to the asynchronous AWGN channel and to multipath fading channels is discussed at the end of section 3.

Now, suppose each user's data is convolutionally encoded and interleaved, where b_j now refers to the code bit of user j during the interval of interest. Throughout the paper we use the half-rate convolutional encoder given by the octal generators 5 and 7 and that has a memory order, as defined in [11], equal to 2. In all BER comparisons, we shall plot the BER against the information bit SNR $\grave{\gamma}$ which is equal to 2γ for the half-rate encoders used. The SNR is equal for all users. Soft-decision Viterbi decoding is applied at the receiver with a truncation depth of at least 5 times the memory order. Due to the variations in deinterleaving delays in the DIP scheme, as described in section 3, the truncation depth is chosen to be larger for some users than others so that the total deinterleaving plus decoding delay is equal for all users.

The computationally simple approach is to carry out the IC operation to completion before performing any error correction. As mentioned in the Introduction, we refer to this approach as Interference Cancellation with Undecoded Decisions (ICUD). A conceptual diagram of this scheme

is shown in Figure 1. A chip-matched filter followed by a sampler provides the samples $r(n)$. The samples $r(n)$ are then element-wise multiplied by the spreading sequence s_k of each user and the accumulators complete the despreading operations. The output of the accumulators is then multiplied by the complex conjugate of each user's phase and the in-phase component is used for subsequent processing as in (2). A hard decision is then made on the code bits of users 2 through K. These decisions are weighted with the fading and crosscorrelation coefficients and then subtracted from the matched filter output of user 1, $y_1(1)$ as described by (3). After IC has been completed, a deinterleaver followed by a soft-decision Viterbi decoder (VD) processes the signal of user 1, $\grave{y}_1(2)$, to produce the final bit decisions $\hat{b}_1(2)$. In a practical receiver the IC is more easily done in the spread domain by respreading the code bit estimate of each user using its spreading sequence and despreading again after the IC is performed.

An alternative, and more complex, structure is the Post-Decoding IC (PDIC) where a bank of single-user VDs prior to the second stage result in better tentative decisions on the *code* bits $\{\hat{b}_j(1)\}$. A bank of interleavers is needed after the first bank of VDs for re-ordering of the MAI terms before IC. A second bank of VDs is of course needed after the IC operation, and therefore a second deinterleaver bank is also required. Figure 2 is a conceptual diagram of the PDIC scheme. Because of more accurate first stage decisions, we expect overall performance, i.e. the BER after the second stage, to be improved relative to ICUD. However, two factors may reduce this performance advantage. In fact, we find that in some special cases ICUD performance is slightly better. The first such factor is the burstiness of the decoding errors made by the first bank of VDs. Such error bursts occur when the VD goes through an error event [11] and the average length of those error bursts is proportional to the average error event length [12]. This causes the RMAI terms in a user's signal after the IC stage to be correlated from one time instant to another. Consequently, the second VD for that user performs poorly due to the introduced channel memory. This problem is similar to that encountered in concatenated coding schemes where the inner decoder produces bursty errors which adversely affect the performance of the outer decoder. Inner and outer interleaver-deinterleaver pairs are used in concatenated coding systems to solve the problem. For PDIC schemes, however, DIP must be assigned to each user as explained in section 3 to overcome the problem of error burstiness. The second factor which hurts PDIC performance is particular to fading channels and has to do with the dependence between the RMAI terms in a user's signal and that user's instantaneous received power. This is best understood by considering a 2-user example, where we are interested in the signal of user 1. For the ICUD scheme, the occurrence of an error in the first stage decision for the code bit of user 2 is strongly correlated with the occurrence of an instantaneously large user 1 signal ($|c_1|$). Thus, non-zero RMAI terms will usually coincide with a large $|c_1|$, resulting in a higher effective signal to interference ratio at the input to the final VD for user 1. For the PDIC scheme, on the other hand, a first stage decision error for user 2 is part of an *error event*

out of the first VD, and therefore is not *as strongly* correlated with a large $|c_1|$. This results in a slightly lower effective average signal to interference ratio at the input to the final VD. Computer simulation measurements of the expectation of the differential instantaneous energies $(|c_1|^2 - |c_2|^2)$ given a first stage error in one of the two users' decisions demonstrate this effect ([13, Table 3.1] or [14]). Therefore, even though the decision error rate of the first stage is normally lower for the PDIC scheme, the final BER for the ICUD scheme can be lower than the BER of the PDIC scheme with DIP on the fading channel. This occurs, however, in the very restricted case of a small number of users (we have only observed it with 2 and 3 users) on a frequency-nonselective time-uncorrelated Rayleigh fading channel with fixed crosscorrelations (i.e. short spreading sequences) and a high signal to noise-power ratio (SNR) operating point. Such a case is shown in Figure 3 which compares the BER of the PDIC (with DIP) and ICUD receivers for 2-user systems on the fading channel. A similar observation was made in [4, p. 1195] but an alternative explanation was given. For systems with random spreading sequences or on the AWGN channel the PDIC scheme with DIP was found to always outperform the ICUD scheme. For completeness, we also mention that the ICUD receiver is more likely to outperform the PDIC receiver with DIP when hard-decision Viterbi decoding is used. To summarize, the factors that cause the ICUD performance to approach, or in special cases exceed, PDIC performance are: a time-varying channel, a small number of users, deterministic sequences, high SNR, and hard-decision decoding.

Next, we state two additional related results on the performance of two-stage IC detectors. The following fact [15] is a direct consequence of the behavior described above.

Fact 1: *The two-stage detector with the conventional first stage exhibits an irreducible error floor on the frequency non-selective Rayleigh fading channel with two active users if and only if their crosscorrelation* $|r_{12}| > 1/\sqrt{2}$.

Proof: See appendix.

This result also holds for the case of unequal average SNRs. Note that this result is for uncoded systems, and so it naturally holds for coded systems but only when decoding is applied *after* IC, i.e. in ICUD structures. The PDIC scheme, on the other hand, generally exhibits an error floor for 2 user systems. The following result covers the case when more than 2 users are active.

Fact 2: *For the two-stage detector with the conventional first stage, the BER of a user* k *exhibits an irreducible floor on the Rayleigh fading channel if* $|r_{kj}| > 0$ *for some* $j \neq k$ *and* $|r_{jl}| > 0$ *for some* $l \neq k, j$.

Proof: See appendix.

In other words, whenever there are more than 2 non-orthogonal users, there shall be an irreducible BER floor. Note that while this result is proved for the frequency non-selective Rayleigh fading channel it carries over naturally to the case of a frequency-selective, i.e. multipath, Rayleigh fading channel.

The above results, while concerned with the asymptotic case of zero noise power, are indicative of the comparative performance of PDIC and ICUD receivers in SNR regions of practical interest. More specifically, the formal result of Fact 1 supports the intuitive arguments given above for the relative performance of ICUD and PDIC receivers (see also Figure 3). The formal result of Fact 2, on the other hand, indicates that the relative advantage of ICUD diminishes as the number of users increases as will be shown in the performance comparisons of section 4. Furthermore, the 2-user results in themselves have relevance to narrowband communication systems where the interference is similar to that between two users with high crosscorrelation in a CDMA system. In particular, the results indicate that such interference may be effectively removed using an ICUD receiver.

3 The Multiuser Interleaving Scheme

As mentioned in the previous section, despite the lower BER in the first stage of PDIC receivers, the burstiness of the errors made by the first bank of VDs severely degrades the error correcting capability of the second VD bank. To eliminate this problem, we propose a multiuser interleaving scheme where users are assigned DIP [16, 14]. In PDIC receivers, the deinterleaving operation prior to the first VD bank necessitates a re-interleaving of the outputs of the first VD bank to replicate the bit order which existed when the signals of all the users were added together at the base station transmitter. This is required in order to carry out IC in the second stage. As a consequence of the re-interleaving operation, a second deinterleaver is needed for each user prior to the second VD (Figure 2). The reason why DIP are needed is as follows. While the re-interleaving operation at the receiver disperses the error (RMAI) bursts out of the first VD bank, the second deinterleaver before the VD of the user of interest would *restore* the RMAI bursts if all users employed the same interleaving and deinterleaving patterns. We illustrate this by an example after we give a description of the DIP scheme.

In the interleaving scheme we propose, a distinct periodic sequence of delays is applied to the bit stream of each user. Following the formulation in [17], the delay sequence applied in the deinterleaver of some user is

$$\grave{d}_n = (n \text{ modulo } P)D \qquad n = 0, 1, 2, \cdots \tag{4}$$

where D is the separation that is introduced between previously adjacent code bits and P is the period of the delay sequence. The sequence of corresponding delays in the interleaver of the same user is given by

$$d_n = ([(n+1)X] \text{ modulo } P)D \qquad n = 0, 1, 2, \cdots \tag{5}$$

where X is the unique integer in the range $1 \leq X < P$ that satisfies $[(D+1)X]$ modulo $P = P - 1$. When P and $D + 1$ are relatively prime, such an interleaver and deinterleaver pair is realizable and introduces a pure delay of $(P - 1)D$ bits at the deinterleaver output. Such interleaver and

deinterleaver pairs are optimal in the sense that for a desired code bit separation, they achieve both the minimum deinterleaving delay and storage requirement [18].

For practical cellular systems, we need enough distinct (P, D) pairs, i.e. enough distinct interleaver-deinterleaver patterns, to accommodate a large number of users; about 60 in the IS-95 system [9], for example. If we confine the deinterleaving delay between 180 and 210 *code*-bits, for example, and require that $P, D \geq 5$, we obtain the 57 (P, D) pairs shown in Figure 4. We can easily relax the deinterleaver delay constraint to allow for more users and still obtain interleaver sizes similar to those in IS-95 [9], or, if needed, we can assign each of a small number of the interleaving patterns to two users without expecting performance to be affected measurably for such a large system. The central (P, D) pairs generally have a smaller deinterleaver delay variation than the extremal (P, D) pairs (upper left and bottom right of Figure 4). Furthermore, the extremal (P, D) pairs result in slightly poorer adjacent bit separation but the resulting increase in BER is barely noticeable. Thus, practically speaking, all valid (P, D) pairs are acceptable.

We now demonstrate the need for DIP through an example of an 8-user system where the users are assigned the interleaving patterns generated by the central (P, D) pairs joined by a line in Figure 4. Figure 5 plots the output of the deinterleaver of user 1 during a time interval of 100 code bits when the input sequences are interleaved by the pattern of user 6. The deinterleaver output is indicated by the position of the output code bit in the original sequence before interleaving. The solid line gives the output when the input sequence is interleaved by the pattern of user 1, in which case the output will simply be the original sequence delayed by 210 code bits, which is the deinterleaver delay for user 1 in this example. Observe that any error (RMAI) bursts in the signal of user 1 will remain intact except if the interleaver patterns of the other users are different from that of user 1.

Since we are proposing the PDIC structure with DIP mainly for the base station receiver due to limitations on the mobile terminal complexity (presently, at least), one point that needs to be clarified is the need for DIP on the asynchronous uplink, since the offsets into the interleaver and deinterleaver tables (i.e. delay sequences) of each user will generally be different with asynchronous transmission. Hence, it would appear that the deinterleaving operation at the input to the second VD would maintain the dispersion of RMAI bursts that occurs due to the re-interleaving operation *even with identical interleaving patterns (IIP)* since the second deinterleaver of the desired user and the second bank of interleavers of the interfering users would effectively be unsynchronized with each other. That is not true, however, because a matched but unsynchronized interleaver and deinterleaver pair, i.e. using the correct patterns but having unequal offsets into their respective delay sequences, produce large contiguous segments of the original sequence. This is illustrated in Figure 6 which shows the deinterleaver output when the interleaving and deinterleaving patterns of user 1 are used, but the deinterleaver sequence is staggered from the interleaver sequence. The large

contiguous segments in the deinterleaver output indicate that the RMAI bursts would hardly be dispersed going into the second VD if IIP are assigned to all users. This example illustrates the need for DIP in asynchronous transmission. For the multipath channel, more than one implementation is possible. For example, a Rake combiner could be implemented for each user before the first deinterleaver. After the VD and interleaver bank re-spread estimates of the multiple paths due to each user are subtracted from the composite received signal. Then, for each user the estimate of its contribution is added back again and a Rake combiner is applied prior to the second deinterleaver and second VD. Again the bursty nature of the RMAI terms persists in the multipath channel if the IIP scheme is applied. We therefore conclude that, at least in principle, the DIP is needed in PDIC receivers for asynchronous multipath fading channels.

Next, we consider the receiver complexity of PDIC structures employing DIP. First, we contrast the complexity of PDIC and ICUD receivers in general. In many practical systems, the VDs process the data on a frame-by-frame basis, i.e. the decoder starts producing decisions after the whole data frame has been received. Hence, with appropriate data buffering the same hardware can be used for the first and second VD banks, with possibly some increase in the memory buffer requirements. The same argument applies for the two deinterleavers required for each user since they are applied before the first and second decoding operations, i.e. they are not applied simultaneously. Depending on the implementation, the interleavers that are required at the receiver in PDIC structures, but not in ICUD structures, may require additional circuitry. Fixed-function hardware blocks typically have a few registers for configurable parameters. If such an implementation is used for the interleaver and deinterleaver functions, then the interleaver may be implemented by the same hardware block used for the deinterleaver since both operations are not applied simultaneously. PDIC receivers also require a convolutional encoder to re-encode the bit streams before IC but the complexity of the encoder is much smaller than that of the decoder. We also mention that software implementation of the above functions on a digital signal processor results in no increase in hardware complexity for PDIC structures relative to ICUD structures but such an implementation will not meet the real-time requirements of some applications.

We now consider the complexity of the DIP scheme versus the IIP scheme in PDIC receivers. In the DIP scheme the interleaving and deinterleaving functions vary by user. If these functions are implemented in software or in configurable hardware as described above, then the complexity of the receivers using the DIP or IIP schemes is the same. Otherwise, different interleaver and deinterleaver functions must be hardwired on each user's transceiver card (in the base station), making it impractical to manufacture, albeit at no increase in the hardware complexity.

From the above discussion it is clear that the relative complexity of the PDIC and ICUD structures and the DIP and IIP schemes depends heavily on the implementation. In practical systems, the VD bank is usually implemented with some form of hardware accelarator due to speed require-

ments. The interleavers and deinterleavers on the other hand may be implemented completely in software. For such a system, the PDIC receiver will have twice the hardware decoding complexity of the ICUD receiver for streaming applications, and will have roughly the same hardware complexity as the ICUD receiver if the decoding is frame-based. In such a system the DIP scheme will not cause additional hardware complexity since the interleaving and deinterleaving functions are implemented in software.

4 Performance Comparisons

To gain an appreciation of the performance gain of PDIC with DIP, we rely on computer simulations in this section and defer the approximate performance analysis till the next section. Figure 7 compares the performance of the ICUD and PDIC schemes, with DIP and IIP, for 8-user systems with equal crosscorrelations $r = 0.35$ and equal SNR γ on the frequency-nonselective uncorrelated Rayleigh fading channel. The central (P, D) pairs of Figure 4 (connected together with a solid line) are employed by the users. The single-user performance and the performance of the conventional (matched filter) receiver serve as lower and upper bounds, respectively, on the performance of suboptimal multiuser detectors, and are included here for comparison purposes. Using the optimized Gold sequences of length 7 [19] to compare the above detectors for a 4-user system, we found that the *relative* performance of the different receiver structures is the same as for the case of equal crosscorrelations. The BER's of the different users are generally unequal with Gold sequences, however, and so for convenience we consider equal user crosscorrelations from now on.

Figure 8 shows the same comparisons on the AWGN channel where the user crosscorrelations $r = 0.25$. The advantage of PDIC with DIP over ICUD is clear, reaching about 4 orders of magnitude in terms of BER for the AWGN channel, and 2 orders of magnitude for the fading channel. The improvement due to DIP over IIP reaches about 3 dB on the AWGN channel for the SNRs of interest but is not as significant on the uncorrelated fading channel. The DIP advantage is greater on the AWGN channel than it is on the fading channel likely because the RMAI terms due to an error event on the AWGN channel have constant weights throughout the error event, whereas on the time-uncorrelated fading channel the instantaneously varying weights mitigate the error burstiness problem which the DIP scheme eliminates. It is also possible that due to the highly structured MAI on the AWGN channel longer error bursts result compared to the fading channel case, where the MAI is Gaussian. This observation also gives insight into the comparative performance of the DIP and IIP structures for indoor and slowly fading channels, where interleaving depth is not sufficient to decorrelate the Rayleigh fading, as well as channels with strong line of sight. In these channels, the RMAI terms are likely to have similar weights throughout the error event. This results in a greater performance advantage for DIP over IIP than for time-uncorrelated fading channels, which represent

high-mobility applications and insufficient interleaving depth. We mention for completeness that when hard-decision decoding is used instead of soft-decision decoding, the DIP scheme provides more significant performance gains on fading channels with 8 active users (not shown).

We now consider systems with random spreading sequences, where we use the spreading factor $\grave{N}$, the number of chips per *information* bit, for comparisons since this figure represents the overall bandwidth spreading regardless of the code rate. The spreading factor N, defined as the number of chips per *code* bit, is used in the approximate analysis due to its suitability. For the half-rate encoders considered in this paper, $\grave{N} = 2N$. Figures 9 and 10 compare the performance of the different receiver structures for systems with random spreading sequences under different loading conditions ($K/\grave{N}$) on the frequency-nonselective Rayleigh fading and AWGN channels, respectively. For the AWGN channel and the given loads, the PDIC scheme with DIP outperforms the ICUD by up to 3 orders of magnitude and DIP outperforms IIP by 1 to 2 orders of magnitude on the BER. On the fading channel, however, the BER improvement from PDIC is roughly between 1 and 2 orders of magnitude, and the difference between DIP and IIP is insignificant. Varying the number of users K while keeping the load $K/\grave{N}$ fixed gave almost identical results (not shown here) for both the fading and AWGN channels. As in the case of systems with deterministic, or short, spreading sequences, the gains due to PDIC and DIP on the fading channel are smaller than on the AWGN channel. The only difference in relative performance trends between systems with deterministic and random code sequences appears in the case of a very small number of users , e.g. 2 or 3, on the fading channel where the PDIC scheme suffers from the problems discussed in section 2 for the case of deterministic sequences.

A question arises at this point about the interleaving size needed to realize the best performance possible with PDIC schemes. Again, this depends on the number of users and type of channel. For memoryless channels, as the number of users increases the interleaver size needed to realize the best possible PDIC performance gets smaller. On the other hand, larger interleavers are generally needed for the AWGN channel than for the Rayleigh fading channel. Both of these observations are consistent with our understanding of the RMAI burstiness which the DIP scheme attempts to mitigate. As an example, for the 8-user systems we studied, interleavers from the set shown in Figure 4 with deinterleaving delays $(P-1)D$ between 180 and 210 bits result in virtually equal performance to that from much larger interleavers whose deinterleaving delays $(P-1)D$ are allowed to be between 1530 bits and 1560 bits. The interleaver sizes needed in a practical system, e.g. IS-95 [9], will be dictated, however, by the correlated fading characteristics of the channel since larger interleavers than those of Figure 4 are needed for that problem. We also studied performance in various near-far situations, and found the relative performance of the investigated methods to be almost identical to the case where all users had equal average energies.

In conclusion, we point out two factors which may increase the importance of DIP in practical

systems. The first is the fact that the constraint length of the codes typically used in practice is larger than the memory order 2 encoders we used. For example, the encoder specified in the reverse link of IS-95 [9] has a memory order of 8. The average burst error length out of the VD considerably increases with memory order [12], which means that the need for DIP will be greater. The second factor is that the interleavers will not result in completely uncorrelated fading especially for slowly fading and strong line of sight channels. This again is expected to increase the average error burst length as well as the average number of error bursts out of the first VD bank. In any case, the DIP scheme does not significantly complicate the PDIC receiver when compared to the IIP scheme as discussed at the end of section 3.

5 Analytical BER Approximations

As explained in section 5.2, which covers the performance analysis of ICUD receivers, it is quite difficult to obtain an exact expression for the BER of a two-stage detector (TSD) with the conventional first stage when hard decisions are used for subtraction of the MAI. This is also the case when attempting to obtain the pairwise error probability (PEP) after the second stage in an ICUD receiver. The PEP, P_d, is the probability that the VD selects an incorrect path over the correct path at some point in the decoding trellis where the two paths are apart by a Hamming distance of d. In this section we, therefore, derive approximations to the probability of error for the various TSD structures considered. For coded systems, the PEP is first obtained and then used in a union bound to give an approximation, or an upper-bound if the PEP is exact, to the BER. We start with an analysis of the first stage, for which some exact results may be obtained. The analysis is carried out mainly for the frequency-nonselective Rayleigh fading channel. For the asynchronous AWGN channel, a detailed approximate analysis of multi-stage detectors has been carried out in [20], primarily for uncoded systems but also covering the ICUD structure briefly. In [2], a more exact analysis was performed also for the asynchronous AWGN channel and uncoded systems, but the probability of error expressions derived require numerical evaluation. Similar results by the same authors are given for synchronous uncoded systems in [21].

5.1 First Stage Analysis

We consider first the case where the users employ deterministic, or short, spreading sequences. Hence, the user crosscorrelations $\{r_{jk}\}$ are fixed for all bit intervals. In that case, we have the following expressions [15] for the BER of the uncoded system and the PEP for the convolutionally encoded system.

Fact 3: *For K users with fixed crosscorrelations transmitting synchronously on a frequency nonselective Rayleigh fading channel with perfect interleaving, the matched filter (conventional) receiver*

followed by a soft-decision VD with perfect CSI (channel state information) has the following exact pairwise error probability (for user 1)

$$P_d = q_1^d \sum_{i=0}^{d-1} \begin{pmatrix} d-1+i \\ i \end{pmatrix} (1-q_1)^i \tag{6}$$

where

$$q_1 = \frac{1}{2}\left[1 - \sqrt{\frac{\gamma_1}{\gamma_1 + \sum_{j=2}^{K} \gamma_j r_{1j}^2 + 1}}\right] \tag{7}$$

is the error probability with no error correction and $\gamma_j = \frac{1}{2}\frac{\mathbf{E}[|c_j|^2]}{\sigma^2}$ *is the average SNR of user* j.

Proof:

We seek first to show that the MAI terms in (2) are independent. Due to the independence of the bits and fading coefficients of the users, the MAI terms in (1) are independent zero-mean complex Gaussian random variables. Taking $k = 1$ in (2), we observe that while θ_1 is common to all MAI terms, we can prove (by calculating the joint densities) that $\{\beta_{j1} = cos(\theta_j - \theta_1)\}$ remain independent due to the modulo-2π nature of the phase, and have the same PDF (Probability Density Function) as $\{\cos(\theta_j)\}$ [1]. Therefore, $\{|c_j|\beta_{j1}\}$ are independent Gaussian random variables.

Now, we desire to calculate the variance of the MAI terms. Since the MAI terms have zero mean, the variance of the MAI term representing the contribution of user j is equal to $\mathbf{E}[b_j^2 r_{1j}^2 |c_j|^2 \beta_{j1}^2]$. Since $|c_j|\beta_{j1}$ is zero-mean Gaussian with variance equal to $\frac{1}{2}\mathbf{E}[|c_j|^2]$, the desired variance is given by $\frac{1}{2}\mathbf{E}[|c_j|^2] r_{1j}^2 = \gamma_j r_{1j}^2 \sigma^2 = \mathcal{E}_j r_{1j}^2$ where $\mathcal{E}_j$ is the average code bit energy for user j. Since the MAI terms are also independent of the noise term $\grave{n}_1$, the total interference plus noise variance is therefore $\sum_{j=2}^{K} \gamma_j r_{1j}^2 \sigma^2 + \sigma^2$. We can now define an equivalent SNR for user 1, γ_{e1}, given by

$$\gamma_{e1} = \frac{1}{2}\frac{\mathbf{E}[|c_1|^2]}{\sum_{j=2}^{K} r_{1j}^2 \gamma_j \sigma^2 + \sigma^2} = \frac{\gamma_1}{\sum_{j=2}^{K} r_{1j}^2 \gamma_j + 1} \tag{8}$$

Substituting γ_{e1} in the expression for the BER of a single-user on a frequency-nonselective Rayleigh fading channel with additive Gaussian noise [22, Equation 14-3-7] we obtain the BER of user 1 for an uncoded system

$$q_1 = \frac{1}{2}\left(1 - \sqrt{\frac{\gamma_{e1}}{1+\gamma_{e1}}}\right) \tag{9}$$

Substituting (8) into (9) we arrive at the form given in (7).

For the PEP, we note that P_d for a single user on a frequency-nonselective Rayleigh fading channel is equal to the error probability for a user employing d^{th}-order diversity with maximum ratio combining at the receiver but with no error-control coding. That error probability is given by [22, Equation 14-4-15]. Substituting the equivalent SNR, γ_{e1}, we obtain P_d as given in (6). Alternatively, we could derive (6) by expressing the VD branch metric as a Hermitian quadratic

[1] The PDF of β_{jk} for all j and k can be shown to be given by $f_\beta(x) = \frac{1}{\pi\sqrt{1-x^2}}, \quad -1 < x < 1$.

form in complex Gaussian variates and utilizing the distribution properties of such a form ([23, Appendix B]). That derivation is given in [13]. $\diamondsuit$

It should be emphasized that no approximation is used in the BER expressions given in Fact 3, i.e. the uncoded BER and PEP for the first stage are exact. Having obtained the PEP P_d we now seek the *code*-bit error probability, p_1, out of the first stage VD bank. This will be needed for the BER analysis of PDIC systems which depends explicitly on the first stage error probability. A different approach is taken for the analysis of ICUD receivers. For the first stage error probability, we use the union bound to obtain an upper bound on the code bit error rate, p_1. Thus, for a half-rate convolutional encoder, using simple probability arguments we can write

$$p_1 < \sum_{d=d_f}^{\infty} \frac{1}{2} d A_d P_d \tag{10}$$

where A_d is the number of weight d paths. The first 18 terms are often used in the literature to compute the bound in (10), e.g. [24], but fewer terms are usually sufficient to compute the bound quite accurately, unless the crosscorrelations r_{1j} are very high.

For systems with random spreading sequences $r_{1j} = \frac{1}{N}\sum_{l=1}^{N} s_{1l}s_{jl}$, where s_{jl} is the $l-$th chip in the spreading sequence of user j and is equal to ± 1 with equal probability. The spreading factor, N, is equal to the number of chips per code bit. In the case of random sequences, the MAI terms are not exactly Gaussian, but the total MAI plus noise can be modeled, accurately in many cases, by a Gaussian random variable. This approach, sometimes referred to as the Standard Gaussian Approximation (SGA), is based on application of the Central Limit Theorem (CLT) - see any probability text - to the sum of identically distributed zero-mean, albeit dependent in this case, random variables. The dependence between the MAI terms is due to the dependence between the crosscorrelations $\{r_{1j}\}$, which are nevertheless pairwise uncorrelated [20]. Except for certain values of K and N, however, the dependence between the MAI terms is quite mild and the SGA applies well. For calculation of the variance of the total MAI and noise, it can be easily shown that $\mathbf{E}[r_{1j}^2]$ evaluates to $1/N$. Since the MAI terms are pairwise uncorrelated and have zero mean, we can simply add the variances of all terms to obtain the desired variance. The resultant equivalent user 1 SNR is therefore given by (8) with r_{1j}^2 replaced by $1/N$. For the case of equal user energies, $\gamma_j = \gamma$, we obtain the following familiar approximation for the equivalent SNR

$$\gamma_e \approx \left(\frac{K-1}{N} + \frac{1}{\gamma} \right)^{-1} \tag{11}$$

which can then be used to obtain the BER and PEP by substituting in (9) and (6),respectively. Computer simulation results, not shown here, verify the accuracy of the above approximation for uncoded systems for a wide range of values of K and N while for convolutionally encoded systems the accuracy is not as high, particularly for small K and large N[13].

5.2 Second Stage Analysis: ICUD

The difficulty in obtaining a closed-form expression for the BER of a TSD with a conventional first stage making hard decisions lies in computing the probability distribution of the RMAI plus noise. This can be seen by writing out the expression for the RMAI due to user j in the signal of user 1, which we denote by ζ_j, as follows

$$\zeta_j = r_{1j}|c_j|\beta_{j1}\{b_j - \mathrm{sgn}[|c_j|b_j + \sum_{l\neq j} r_{jl}|c_l|\beta_{lj}b_l + \grave{n}_j]\} \tag{12}$$

The strong nonlinearity due to the hard decisions at the first stage precludes the matrix-type formulations possible with linear (soft) IC schemes. Adding to the difficulty are the following dependencies between the RMAI terms $\{\zeta_j\}$ and the instantaneous signal strength $|c_1|$ of the user of interest:

- The RMAI terms $\{\zeta_j\}$ are dependent because of the $\{|c_l|\}$ random variables common to all, the mutual dependence between the noise terms $\{\grave{n}_j\}$, and, for random sequences, the dependence among $\{r_{kj}\}$.
- $\zeta = \sum_j \zeta_j$ and $\grave{n}_1$ are dependent because of the mutual dependence between the noise terms $\{\grave{n}_j\}$.
- $|c_1|$ and ζ are dependent because of the direct dependence of each element of $\{\zeta_j\}$ on $|c_1|$.

We, therefore, resort to approximating the RMAI, ζ, as a Gaussian random variable by invoking the Central Limit Theorem for dependent variables [25] since ζ is the sum of the zero-mean identically distributed, albeit dependent, random variables $\{\zeta_j\}$. In general, the conditions under which the CLT may be successfully applied to a sum of dependent random variables are quite mild, but they are difficult to verify [25]. We shall, therefore, presuppose the applicability of the CLT to the RMAI and subsequently verify the accuracy of the resultant approximations using computer simulations. Modelling the *MAI* as Gaussian has been used in the analysis of CDMA systems for a long time, e.g. [26], where the total MAI variance is computed as the sum of the variances of the individual MAI terms. However, due to the dependence relations described above for the RMAI terms, the estimation of the variance will be more involved in this case.

We now seek to obtain $\mathbf{Var}[\zeta_j]$ which is equal to $\mathbf{E}[\zeta_j^2] = \mathbf{E}[(2r_{1j}|c_j|\beta_{j1}e_j)^2]$ since $\mathbf{E}[\zeta_j] = 0$ from symmetry arguments. Note that each of $\beta_{j1}, |c_j|$, and, for random sequences, r_{1j} is pairwise dependent with e_j. Fortunately, these dependencies are not very strong and can be ignored except for the dependence between $|c_j|$ and e_j. Thus, we approximate the desired variance by $\mathbf{Var}[\zeta_j] \approx 4\ \mathbf{E}[r_{1j}^2]\ \mathbf{E}[\beta_{j1}^2]\ \mathbf{E}[(|c_j|e_j)^2]$. From basic probability we can show that $\mathbf{E}[\beta_{jk}^2] = 1/2$ and, for random sequences, $\mathbf{E}[r_{1j}^2] = 1/N$. Finally, the last remaining term in the variance formula evaluates to (see

the Appendix for proof)

$$\mathbf{E}[(|c_j|e_j)^2] = \mathcal{E}_j \left[1 - \sqrt{\frac{\mathcal{E}_j}{\mathcal{E}_j + \eta_j^2}} \left(\frac{3\eta_j^2 + 2\mathcal{E}_j}{2\eta_j^2 + 2\mathcal{E}_j}\right)\right] \tag{13}$$

where

$$\eta_j = \sum_{l \neq j} \mathcal{E}_l r_{jl}^2 + \sigma^2 \tag{14}$$

for short (deterministic) sequences, and

$$\eta_j = \frac{1}{N} \sum_{l \neq j} \mathcal{E}_l + \sigma^2 \tag{15}$$

for long (random) sequences and η_j^2 represents the variance of the MAI plus noise as seen by user j at the first stage output. In obtaining the variance of the total RMAI plus noise, we can once more ignore the mutual dependence, which is not very strong, between the RMAI terms $\{\zeta_j\}$ and the thermal noise term $\grave{n}_1$ of our user of interest. Thus, the variance of the total RMAI plus noise seen by user 1 is given by $\Psi_1 = \mathbf{Var}[\zeta + \grave{n}_1] \approx \mathbf{Var}[\zeta] + \sigma^2$ which may be expressed as

$$\Psi_1 \approx 2 \sum_{j=2}^{K} r_{1j}^2 \mathcal{E}_j \left[1 - \sqrt{\frac{\mathcal{E}_j}{\mathcal{E}_j + \eta_j^2}} \left(\frac{3\eta_j^2 + 2\mathcal{E}_j}{2\eta_j^2 + 2\mathcal{E}_j}\right)\right] + \sigma^2 \tag{16}$$

and r_{1j}^2 is replaced by its expectation $1/N$ for the case of random sequences. We can now define an equivalent (single-user) SNR after the IC for user 1 as

$$\gamma_{e1}(2) = \frac{\mathbf{E}[|c_1|^2]}{2\Psi_1} = \frac{\mathcal{E}_1}{\Psi_1} \tag{17}$$

Substituting $\gamma_{e1}(2)$ in Equation (9), we obtain an approximation to the uncoded BER of user 1 after the IC of the second stage

$$q_1(2) \approx \frac{1}{2} \left(1 - \sqrt{\frac{\gamma_{e1}(2)}{1 + \gamma_{e1}(2)}}\right) \tag{18}$$

It should be mentioned that by using Equation (9), we have ignored the dependence between ζ and each of $|c_1|$ and b_1, since the derivation of (9) involves conditioning on both $|c_1|$ and b_1 and then taking the expectation. Strictly speaking, conditioning on either of $|c_1|$ and b_1 affects Ψ_1, which would be a conditional variance in this case. In fact, conditioning on b_1 introduces a bias in ζ. This has also been observed on the asynchronous AWGN channel [20]. However, these effects are weak and can be ignored as we shall see in assessing the accuracy of the approximation. For uncoded systems, the approximation is very accurate for systems with deterministic and random sequences, in contrast to an approximation that ignores the dependence between $|c_j|$ and e_j in estimating the variance Ψ_1 [13]. To obtain the PEP at the output of the second VD, $P_d(2)$, we substitute $q_1(2)$

in place of q_1 in Equation (6). Finally, we use a union bound to obtain an approximation to the information bit error rate for the ICUD scheme

$$P_b \approx \sum_{d=d_f}^{\infty} B_d \; P_d(2) \tag{19}$$

where B_d is the total number of nonzero information bits on all weight d paths. Note that the union bound thus applied is no longer an upper bound due to the approximations involved in arriving at the PEP.

Figures 11 and 12 compare the approximated BER and that obtained by simulations for coded systems (ICUD) with 8 users having $r = 0.15$ and $r = 0.25$, respectively, and equal received energies. Also shown in the figures is the approximate BER obtained when the dependence between $|c_j|$ and e_j is ignored. In the figures, we refer to this approximation as the "first approximation" and to our approximation as the improved approximation. In both figures, the improved approximation is clearly more accurate. The weakness of the approximations at low SNR is due to the well-known looseness of the union bound. Eliminating a few significant terms from the summation (19) of the Union Bound (UB) improves the accuracy at low SNR without usually affecting the bound at high SNR. The approximate BER using the first 5 terms of the UB is shown in Figure 11. The same technique has been used elsewhere in the literature, e.g. [24, Figures 2 and 3] where only the first 6 terms of the UB are used.

For systems with long sequences and a spreading factor N, the BER performance is much worse than that of systems using fixed sequences having $r^2 = 1/N$. This is true when subtractive IC is applied with error correction, whether the ICUD or the PDIC scheme is used. Hence, the approximation is not valid for IC structures with long sequences when coding is used. This can be explained by the very poor suitability of the standard VD branch metric for the RMAI statistics in this case. In fact, based on this observation, in [27] we model the RMAI as Gaussian with time-dependent variance, and by applying modified VD branch metrics that are a function of the time-varying crosscorrelations, we obtain improved performance.

5.3 Second Stage Analysis: PDIC

The foregoing improved variance estimate was possible for ICUD systems because we could easily express e_j directly in terms of known parameters (refer to (12) and (3)). For PDIC systems, on the other hand, the first stage errors made by the single-user VDs are due to error events, and a computation as in (13) is not possible. However, the dependence between e_j and $|c_j|$ at any given instant is also much weaker than in the ICUD case, as we mentioned earlier in our discussion about the observed RMAI bias (section 2). Thus, we estimate the desired variance by $\mathbf{Var}[\zeta_j] = \mathbf{E}[\zeta_j^2] \approx 4\ \mathbf{E}[r_{1j}^2]\ \mathbf{E}[\beta_{j1}^2]\ \mathbf{E}[|c_j|^2]\mathbf{E}[e_j^2] = 4\ \mathbf{E}[r_{1j}^2]\ \mathcal{E}_j\ p_j$ where p_j is the first stage code bit error rate, which can be upper-bounded (tightly in most cases) using (10). As we did for the ICUD

case, the variances of the individual RMAI terms and noise are added to obtain

$$\Psi_1 \approx 4 \sum_{j=2}^{K} \mathbf{E}[r_{1j}^2] \; \mathcal{E}_j \; p_j + \sigma^2 \tag{20}$$

The remaining steps are identical to those for the ICUD scheme. Namely, we use (17), (18), (6), and (19) to obtain the information BER. For the IIP implementation of PDIC, the analysis is further complicated by the correlations between $\{\zeta_j\}$ from one time instant to another due to the burstiness of errors out of the first VD bank. We, therefore, rely on computer simulations to measure the BER for the IIP case.

Figure 13 shows the approximate and measured BER for an 8-user system with $r = 0.25$ and equal energies using the PDIC structure with DIP. As we did for the ICUD scheme, eliminating a few significant terms from the UB summation improves the accuracy at low SNR. In this case, using the first 3 terms of the UB gives the best agreement with simulations. It is interesting to note that the approximation agrees reasonably with simulations considering the fact that we apply the union bound twice. This is because the approximation errors are not of the same polarity: For high crosscorrelations r_{1j}, the first application of the union bound is a loose upper bound on p_1, the first stage code bit error probability for user 1, since the MAI variance is high even as $\gamma \to \infty$. Yet, as r_{1j} increases, the Gaussian approximation underestimates the error probability. The fact that the SGA gives optimistic BER results is well-known for uncoded systems and this is more accentuated for systems with error control coding because the VD branch metric is optimized for additive Gaussian noise. On the other hand, for low r_{1j} the union bound becomes a tighter upper bound as γ increases while the Gaussian approximation underestimates the BER less severely.

It should be mentioned that in [28] reasonable agreement was obtained between the BER measured by simulation and the estimate obtained by applying a Gaussian approximation equivalent to ours for PDIC systems with random sequences. However, asynchronous systems were considered in that study, and the agreement was demonstrated for successive IC. The statistics of the RMAI are quite different for asynchronous systems, and are more easily modeled as Gaussian, than they are for synchronous systems. Furthermore, successive schemes have a combination of MAI and RMAI terms in any user's signal (except the last which only has RMAI terms), and MAI is better approximated as Gaussian than RMAI. Finally, it should be pointed out that for heavily loaded systems these approximations may be poor due to the high crosscorrelation between the RMAI terms and hence the inaccuracy of the variance estimate. In such cases we rely on computer simulations for performance evaluations.

6 Conclusions

In this paper, we studied two alternative structures, which we called the ICUD and PDIC schemes, for subtractive IC receivers used to demodulate convolutionally-encoded CDMA systems. We compared the performance of synchronous systems on both AWGN channel and the frequency-nonselective time-uncorrelated Rayleigh fading channel. We also discussed the cases of the asynchronous AWGN and multipath fading channels. We found that while PDIC usually has better performance than ICUD, it is possible, albeit in very special cases, for the ICUD receiver to outperform the PDIC receiver. We studies the RMAI terms and concluded that the PDIC scheme does not realize its full potential unless DIP are employed by different users. We proposed such a multiuser interleaving scheme for practical systems and significant improvements were realized on the AWGN channel. The gain due to DIP increased with higher SNR indicating that it pushed the BER floor due to the conventional first stage lower. On the flat time-uncorrelated fading channel, improvements due to DIP were more modest. However, we pointed out that DIP is important in indoor and slow fading scenarios, or whenever the interleaving depth is insufficient to completely decorrelate the fading. Furthermore, the larger constraint length of the encoders used in practical systems compared to the encoders used in our simulations results in longer error bursts out of the first VD bank, and hence a greater need for the DIP scheme. The applicability of the DIP scheme to receivers with Rake combining for multipath fading channels was also demonstrated. Nevertheless, further work is needed to verify and quantify such improvements on practical fading channels. The complexity of both PDIC and ICUD structures was compared. It was shown that the added hardware complexity of PDIC structures is not significant and its dependency on the implementation was discussed.

Existence of the BER floor in systems employing ICUD was investigated. The implications of these findings for practical, including narrowband, systems were discussed. In particular, we conclude that for systems with a small number of interfering users, ICUD receivers might be more suitable than PDIC receivers.

A family of approximations, and some exact results, were derived for the error probability of various receiver structures considered in the paper. In particular, a novel estimate of the RMAI variance was derived resulting in a better approximation to the BER of ICUD receivers. The applicability of the Gaussian-based approximations was assessed for the various receivers under different conditions. As expected, the approximations were inaccurate for heavily loaded systems.

7 Appendix

Proof of Fact 1: Without loss of generality, assume $b_1 = -1$. Equation (3) in the zero-noise case

now becomes

$$\dot{y}_1(2) = |c_1|(-1) + 2r_{12}\beta_{21}|c_2|e_2 \tag{21}$$

and an error will occur when $\dot{y}_1(2) > 0$. Call this the event E. Thus, $\{E\} \Leftrightarrow \{2r_{12}\beta_{21}|c_2|e_2 > |c_1|\}$. From this we have,

$$\{E\} \Rightarrow \{2|r_{12}\beta_{21}||c_2| > |c_1|\} \tag{22}$$

since $|e_2| \leq 1$, and

$$\{E\} \Rightarrow \{e_2 \neq 0\} \tag{23}$$

as well. But $\{e_2 \neq 0\}$ means, by definition, that $\hat{b}_2(1) \neq b_2$. Since $\hat{b}_2(1) = \text{sgn}[|c_2|b_2 - r_{12}|c_1|\beta_{12}]$, then $\{e_2 \neq 0\} \Rightarrow \{b_2 \neq \text{sgn}[|c_2|b_2 - r_{12}|c_1|\beta_{12}]\}$. Thus, $\{e_2 \neq 0\} \Rightarrow \{|c_2| < |r_{12}\beta_{12}||c_1|\}$. But, we proved that $\{E\} \Rightarrow \{e_2 \neq 0\}$. Thus,

$$\{E\} \Rightarrow \{|c_2| < |r_{12}\beta_{12}||c_1|\} \tag{24}$$

Combining (22) and (24), we can write $\{E\} \Rightarrow \{2|r_{12}\beta_{12}| > \frac{|c_1|}{|c_2|} > \frac{1}{|r_{12}\beta_{12}|}\}$ (since $\beta_{12} = \beta_{21}$). Thus, $\{E\} \Rightarrow \{\beta_{12}^2 > 1/2r_{12}^2\}$.

But $\beta_{12}^2 \leq 1$. Thus, $\{E\} \Rightarrow 1/2r_{12}^2 \leq 1$. Thus, $\{E\} \Rightarrow |r_{12}| \geq 1/\sqrt{2}$. This proves the 'only if' part of the claim.

Now assume that $|r_{12}| \geq 1/\sqrt{2}$. Hence, $1/2r_{12}^2 \leq 1$. Thus $\{\beta_{12}^2 > 1/2r_{12}^2\}$ occurs with non-zero probability. We may now hypothesize $|c_2|$ large enough to satisfy (22) yet small enough to satisfy (24). Finally, we hypothesize polarities such that $\beta_{21}e_2 > 0$ for $r_{12} > 0$ or $\beta_{21}e_2 < 0$ for $r_{12} < 0$. The variables in this hypothesized composite outcome are independent, and cause the event $\{E\}$ to occur. Hence, an error will occur with non-zero probability if $|r_{12}| \geq 1/\sqrt{2}$. This proves the 'if' part of the claim. $\diamondsuit$

Proof of Fact 2: We start with the K=3 case, with positive crosscorrelations. For the zero-noise case, and from (3) and the decision rule for $\hat{b}_1(2)$, it is clear that $\hat{b}_1(2) \neq b_1$, which we call the event E, occurs iff

$$\left| \overbrace{r_{12}|c_2|[b_2 - \hat{b}_2(1)]\beta_{12} + r_{13}|c_3|[b_3 - \hat{b}_3(1)]\beta_{13}}^{(RMAI)_1} \right| > |c_1| \tag{25}$$

and

$$\text{sgn}[(RMAI)_1] \neq \text{sgn}[b_1] \tag{26}$$

This means that $\{E\}$ implies $\{\hat{b}_2(1) \neq b_2\}$, $\{\hat{b}_3(1) \neq b_3\}$, or both. We seek to prove that for at least one of these 3 ways in which $\{E\}$ can occur, $\{E\}$ occurs with a non-zero probability provided $r_{12}, r_{23} > 0$.

Hence, consider the case $\{\hat{b}_2(1) \neq b_2\} \cap \{\hat{b}_3(1) = b_3\}$, and call it the event E_2. From (2) and the decision rule for $\hat{b}_j(1)$, $\{E_2\}$ occurs iff the following 3 conditions are met

$$\left| \overbrace{r_{21}|c_1|b_1\beta_{12} + r_{32}|c_3|b_3\beta_{32}}^{(MAI)_2} \right| > |c_2| \tag{27}$$

and

$$\text{sgn}[(MAI)_2] \neq \text{sgn}[b_2] \tag{28}$$

and

$$\text{sgn}[|c_3|b_3 + r_{32}|c_2|\beta_{23}b_2 + r_{31}|c_1|\beta_{13}b_1] = \text{sgn}[b_3] \tag{29}$$

When $\{E_2\}$ results in $\{E\}$, the conditions described by (25) and (26) become

$$|2r_{12}|c_2|\beta_{12}| > |c_1| \tag{30}$$

$$\text{sgn}[(b_2 - \hat{b}_2(1))\beta_{12}] \neq \text{sgn}[b_1] \tag{31}$$

Hence, the conditions in (27) through (31) occur iff $\{E \cap E_2\}$ occurs.

Now, for any $r_{12} > 0$ we can hypothesize $|c_2|$ large enough to satisfy (30). Similarly, for any $r_{12}, r_{23} > 0$ and any $|c_2|$, we can hypothesize $|c_3|$ large enough to satisfy (27) and (29). For (28) and (31), we hypothesize $b_3, \beta_{32} > 0$, $b_1, \beta_{12} < 0$, and $b_2 < 0$. All the variables in this hypothesized composite outcome are independent. Hence, for any $r_{12}, r_{23} > 0$, $\{E\}$ can occur with non-zero probability.

Since the polarities of the interfering signals and the signal of the user of interest are positive or negative with equal probability and are independent from each other, we can construct similar proofs for all mixtures of positive and negative crosscorrelations. Thus, for any $|r_{12}|, |r_{32}| > 0$, event $\{E\}$ occurs with a non-zero probability. The proof may be easily generalized to the K-user case by hypothesizing the composite event of all but three users having no first stage error. $\diamondsuit$

Proof of Equation 13 : We derive the desired expectation as follows

$$\mathbf{E}\left[|c_j|^2 e_j^2\right] = \mathbf{E}_{|c_j|}\left(|c_j|^2 \mathbf{E}\left[e_j^2 \middle| |c_j|\right]\right) \tag{32}$$

The conditional expectation can be expressed as

$$\begin{aligned} \mathbf{E}\left[e_j^2 \middle| |c_j|\right] &= \sum_{y \in \{-1,0,1\}} y^2 p(y|x) \\ &= p(-1|x) + p(1|x) \\ &= 2p(-1|x) \end{aligned}$$

where $p(y|x) \stackrel{\triangle}{=} p_{e_j\left||c_j|\right.}(y|x)$ is the conditional probability mass function of e_j given $|c_j|$, and the last step is due to problem symmetry. Now,

$$p(-1|x) \;=\; Pr(b_j = -1, \hat{b}_j = 1|\; x)$$

$$
\begin{aligned}
&= Pr(\hat{b}_j = 1|\ x, b_j = -1)\ Pr(b_j = -1) \\
&= \frac{1}{2} Q(x/\eta_j)
\end{aligned}
$$

where $Q(x) = \frac{1}{\sqrt{2\pi}} \int_x^\infty e^{-t^2/2} dt$, and $\eta_j^2 = \sum_{l \neq j} \mathcal{E}_l r_{lj}^2 + \sigma^2$ is the variance of the MAI seen by user j. Substituting this result back in (32),

$$
\mathbf{E}\left[|c_j|^2 e_j^2\right] = \int_0^\infty x^2\ Q(x/\eta_j)\ f_{|c_j|}(x)\ dx \tag{33}
$$

where $f_{|c_j|}(x) = \frac{x}{\alpha^2}\ e^{-x^2/2\alpha^2}$ is the Rayleigh PDF of $|c_j|$ and $\alpha^2 = \mathcal{E}_j = \gamma_j \sigma^2$. Applying the change of variable $x^2 = A$, the r.h.s. (right hand side) in the above equations can be expressed as

$$
\begin{aligned}
&\int_0^\infty A\ \frac{e^{-A/2\alpha^2}}{2\alpha^2}\ Q(\sqrt{A/\eta_j^2})\ dA \\
&= \int_0^\infty \underbrace{\left(\frac{1}{\sqrt{2\pi}} \int_{\sqrt{A/\eta_j^2}}^\infty e^{-t^2/2}\ dt\right)}_{U}\ \underbrace{\frac{A e^{-A/2\alpha^2}}{2\alpha^2}\ dA}_{dV}
\end{aligned}
$$

Evaluating the above integration by parts, $\int_0^\infty U\ dV = UV\,|_0^\infty - \int_0^\infty V dU$ where U and dV are as indicated. We use Leibniz's theorem for differentiation of an integral to evaluate dU, perform a second integration by parts and after some manipulations, arrive at

$$
\mathbf{E}\left[|c_j|^2 e_j^2\right] = \frac{\alpha^2}{2} - \frac{1}{2\eta_j\sqrt{2\pi}} \left[\int_0^\infty \left(A^{1/2} e^{-cA} + \alpha^2 A^{-1/2} e^{-cA}\right) dA\right] \tag{34}
$$

where $c = \frac{2\eta_j^2 + \alpha^2}{2\eta_j^2 \alpha^2}$. Using the integral form of the Gamma-function $\int_0^\infty t^{n-1} e^{-at} dt = \Gamma(n)/a^n$, where $a, n > 0$, we obtain

$$
\mathbf{E}\left[|c_j|^2 e_j^2\right] = \frac{\alpha^2}{2} - \frac{1}{2\eta_j\sqrt{2\pi}} \left[\frac{\Gamma(3/2)}{c^{3/2}} + \alpha^2 \frac{\Gamma(1/2)}{c^{1/2}}\right] \tag{35}
$$

Using $\Gamma(3/2) = \sqrt{\pi}/2$ and $\Gamma(1/2) = \sqrt{\pi}$, and rewriting c and α in terms of the system parameters, and after some manipulation we arrive at Equation (13).

References

[1] S. Verdu, "Minimum Probability of Error for Asynchronous Gaussian Multiple-Access Channels," *IEEE Transactions on Information Theory*, vol. IT-32, pp. 85–96, Jan. 1986.

[2] M. K. Varanasi and B. Aazhang, "Multistage Detection in Asynchronous Code-Division Multiple-Access Communications," *IEEE Trans. on Comm.*, vol. COM-38, pp. 509–519, April 1990.

[3] T. R. Giallorenzi and S. G. Wilson, "Multiuser ML Sequence Estimator for Convolutionally Coded Asynchronous DS-CDMA Systems," *IEEE Trans. on Comm.*, vol. 44, pp. 997–1008, August 1996.

[4] T. R. Giallorenzi and S. G. Wilson, "Suboptimum Multiuser Receivers for Convolutionally Coded Asynchronous DS-CDMA Systems," *IEEE Trans. on Comm.*, vol. 44, pp. 1183–1196, September 1996.

[5] A. J. Viterbi, "Very Low Rate Convolutional Codes for Maximum Theoretical Performance of Spread-Spectrum Multiple-Access Channels," *IEEE Journal on Selected Areas in Communications*, vol. 8, pp. 641–649, May 1990.

[6] W. T. Sang, K. B. Letaief, and R. S. Cheng, "Combined Coding and Successive Interference Cancellation with Random Interleaving for DS/CDMA Communications," in *IEEE Proc. of Vehic. Tech Conf.*, pp. 1825–1829, Sept. 1999.

[7] J. Robert K. Morrow, "Accurate CDMA BER Calculations with Low Computational Complexity," *IEEE Trans. on Comm.*, vol. 46, pp. 1413–1417, November 1998.

[8] S. Gray, M. Kocic, and D. Brady, "Multiuser Detection in Mismatched Multiple-Access Channels," *IEEE Trans. on Comm.*, vol. 43, pp. 3080–3089, December 1995.

[9] TIA/EIA-95-B, "Mobile Station-Base Station Compatibility Standard for Dual-Mode Spread Spectrum Systems," 1998.

[10] R. M. Buehrer, A. Kaul, S. Striglis, and B. D. Woerner, "Analysis of DS-CDMA Parallel Interference Cancellation with Phase and Timing Errors," *IEEE Journal on Selected Areas in Communications*, vol. 14, pp. 1522–1535, October 1996.

[11] S. Lin and D. Costello, Jr., *Error Control Coding - Fundamentals and Applications*. Englewood Cliffs,NJ 07632: Prentice-Hall, 1983.

[12] J. M. Morris, "Burst Error Statistics of Simulated Viterbi Decoded BPSK on Fading and Scintillating Channels," *IEEE Trans. on Comm.*, vol. 40, pp. 34–41, January 1992.

[13] Ayman Elezabi, *Joint Multiuser Detection and Single-User Decoding for Multiple-Access Communication Systems*. PhD thesis, North Carolina State University, May 2000.

[14] A. Elezabi and A. Duel-Hallen, "Two-Stage Receiver Structures for Coded CDMA Systems," in *IEEE Vehicular Technology Conference*, pp. 1425–1429, May 1999.

[15] A. Elezabi and A. Duel-Hallen, "Conventional-based Two-Stage Detectors in Coded CDMA," in *Proc. of IEEE Int. Symp. on Info. Th.*, p. 282, Aug. 1998.

[16] A. Elezabi and A. Duel-Hallen, "A Novel Interleaving Scheme for Multiuser Detection of Coded CDMA Systems," in *Proc. of 31st Ann. Conf. on Info. Sciences and Systems*, pp. 486–491, 1997.

[17] M. V. Eyuboglu, "Detection of Coded Modulation Signals on Linear, Severely Distorted Channels Using Decision-Feedback Noise Prediction with Interleaving," *IEEE Trans. on Comm.*, vol. COM-36, pp. 401–409, April 1988.

[18] J. L. Ramsey, "Realization of Optimum Interleavers," *IEEE Transactions on Information Theory*, vol. IT-16, pp. 338–345, May 1970.

[19] R. Gold, "Optimal Binary Sequences for Spread Spectrum Multiplexing," *IEEE Transactions on Information Theory*, pp. 619–621, October 1967.

[20] D. Divsalar and M. K. Simon, "Improved CDMA Performance Using Parallel Interference Cancellation." JPL Publication 95-21, Oct. 1995.

[21] M. K. Varanasi and B. Aazhang, "Near-Optimum Detection in Synchronous Code-Division Multiple-Access Systems," *IEEE Trans. on Comm.*, pp. 725–736, May 1991.

[22] J. Proakis, *Digital Communications*. McGraw-Hill, 1995.

[23] M. Schwartz, W. Bennett, and S. Stein, *Communication Systems and Techniques*. McGraw Hill, 1966.

[24] R. D. Cideciyan, E. Eleftheriou, and M. Rupf, "Performance of Convolutionally Coded Coherent DS-CDMA Systems in Multipath Fading," in *Proc. of Globecom*, pp. 1755–1760, 1996.

[25] R. J. Serfling, "Contributions to Central Limit Theory for Dependent Variables," *Annals of Math. Stat.*, vol. 39, no. 4, pp. 1158–1175, 1968.

[26] M. Pursley, "Performance Evaluation for Phase-Coded Spread-Spectrum Multiple-Access Communication-Part I: System Analysis," *IEEE Trans. on Comm.*, vol. COM-25, pp. 795–799, August 1977.

[27] A. Elezabi and A. Duel-Hallen, "Improved Single-User Decoder Metrics for Two-Stage Detectors in DS-CDMA," in *IEEE Proc. of Vehic. Tech Conf.*, pp. 1276–1281, Sept. 2000.

[28] P. Frenger, P. Orten, and T. Ottosson, "Evaluation of Coded CDMA with Interference Cancellation," in *IEEE Vehicular Technology Conference*, pp. 642–647, May 1999.

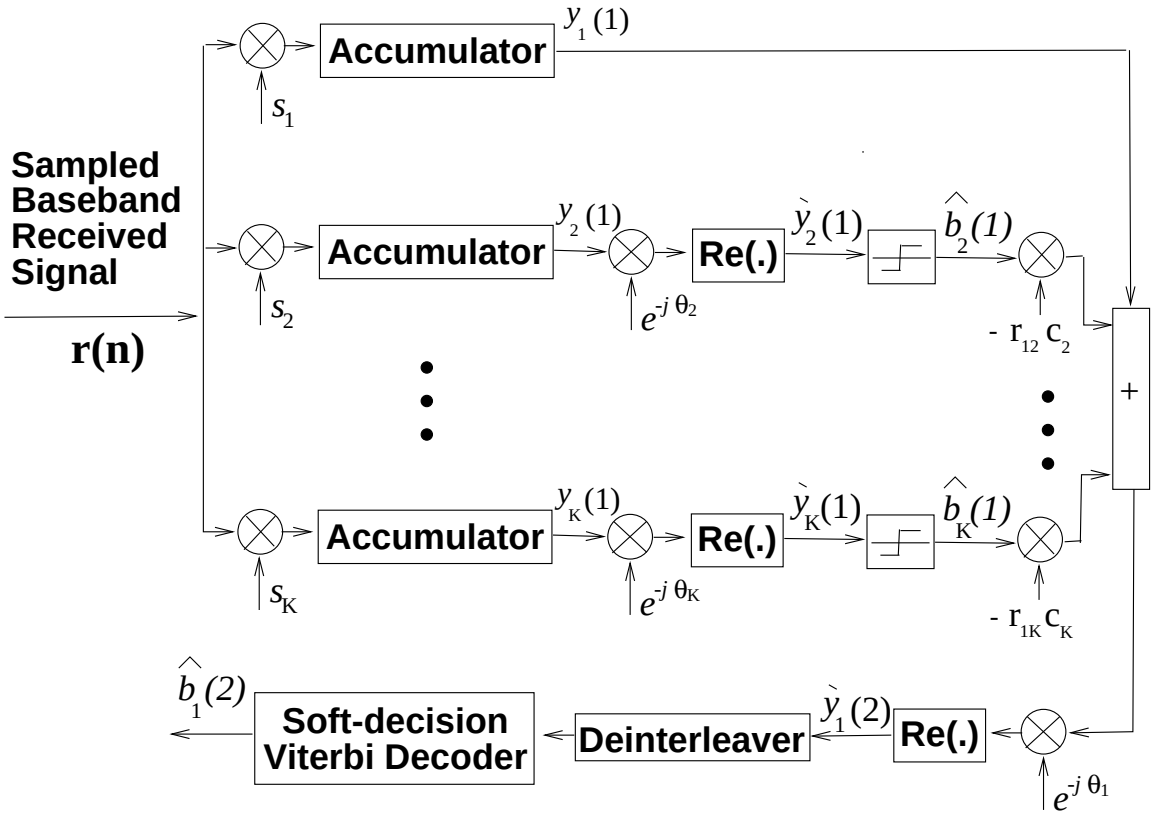

Figure 1: Conceptual Diagram of ICUD (showing IC for user 1 only).

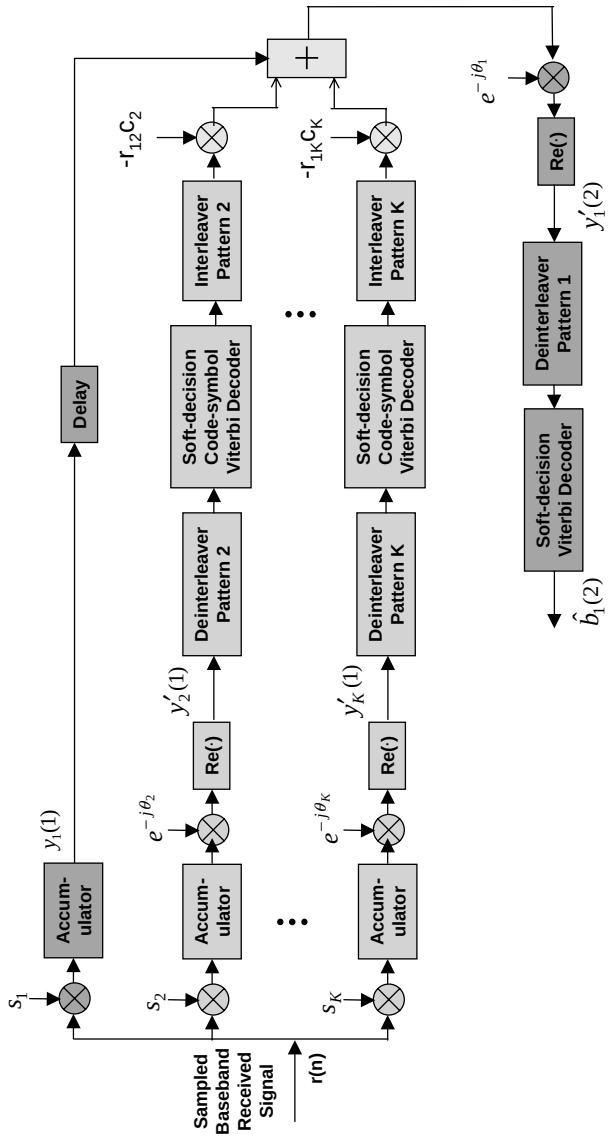

Figure 2: Conceptual Diagram of PDIC (showing IC for user 1 only).

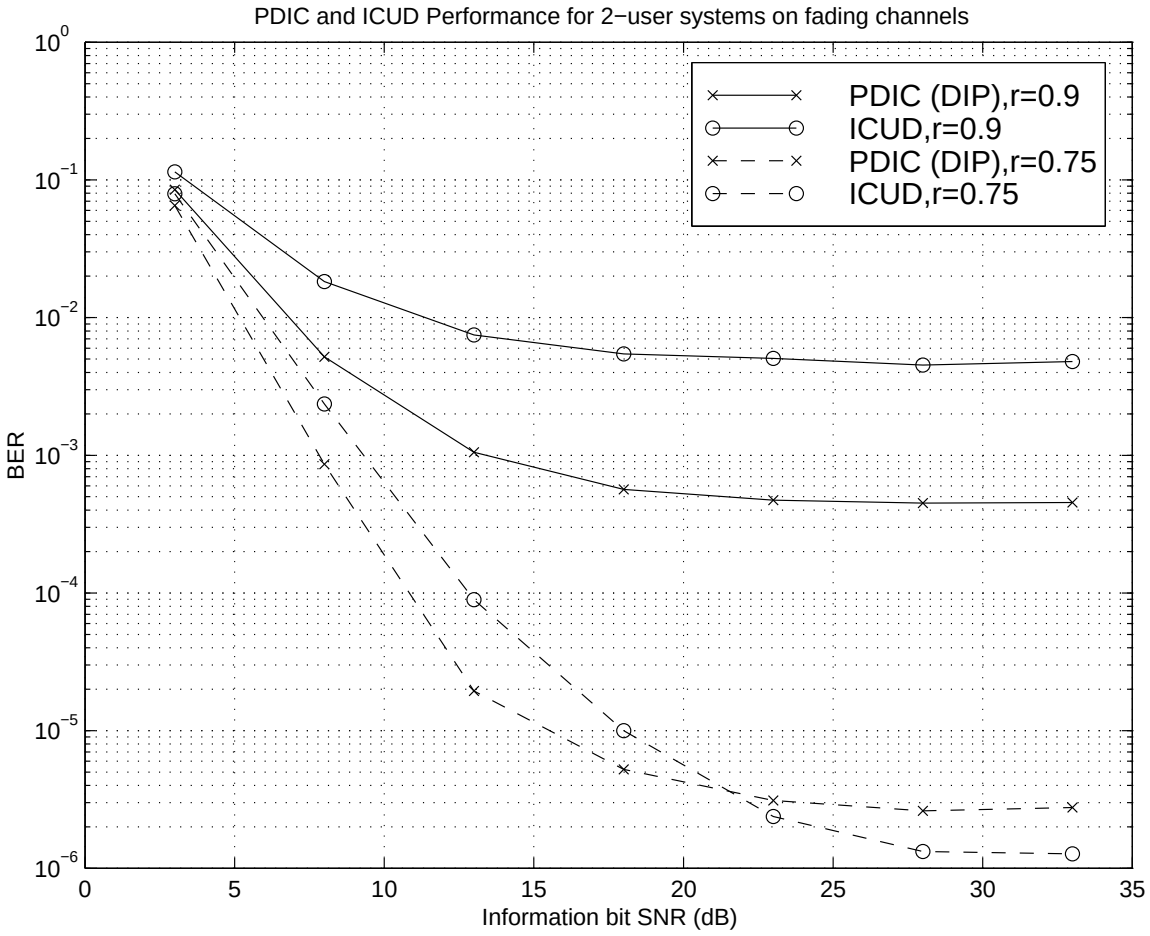

Figure 3: PDIC versus ICUD on a flat frequency-nonselective Rayleigh fading channel for 2-user systems

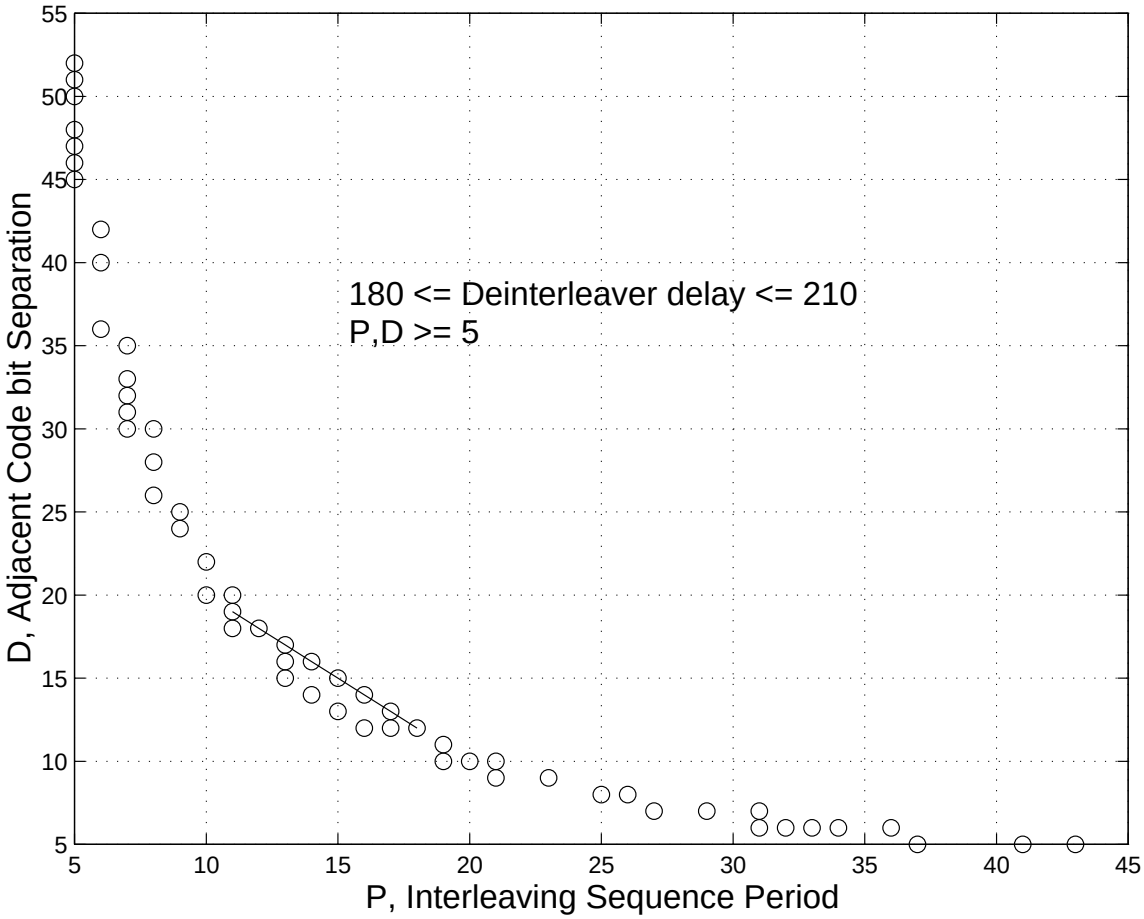

Figure 4: 57 useful (P, D) pairs for DIP in PDIC

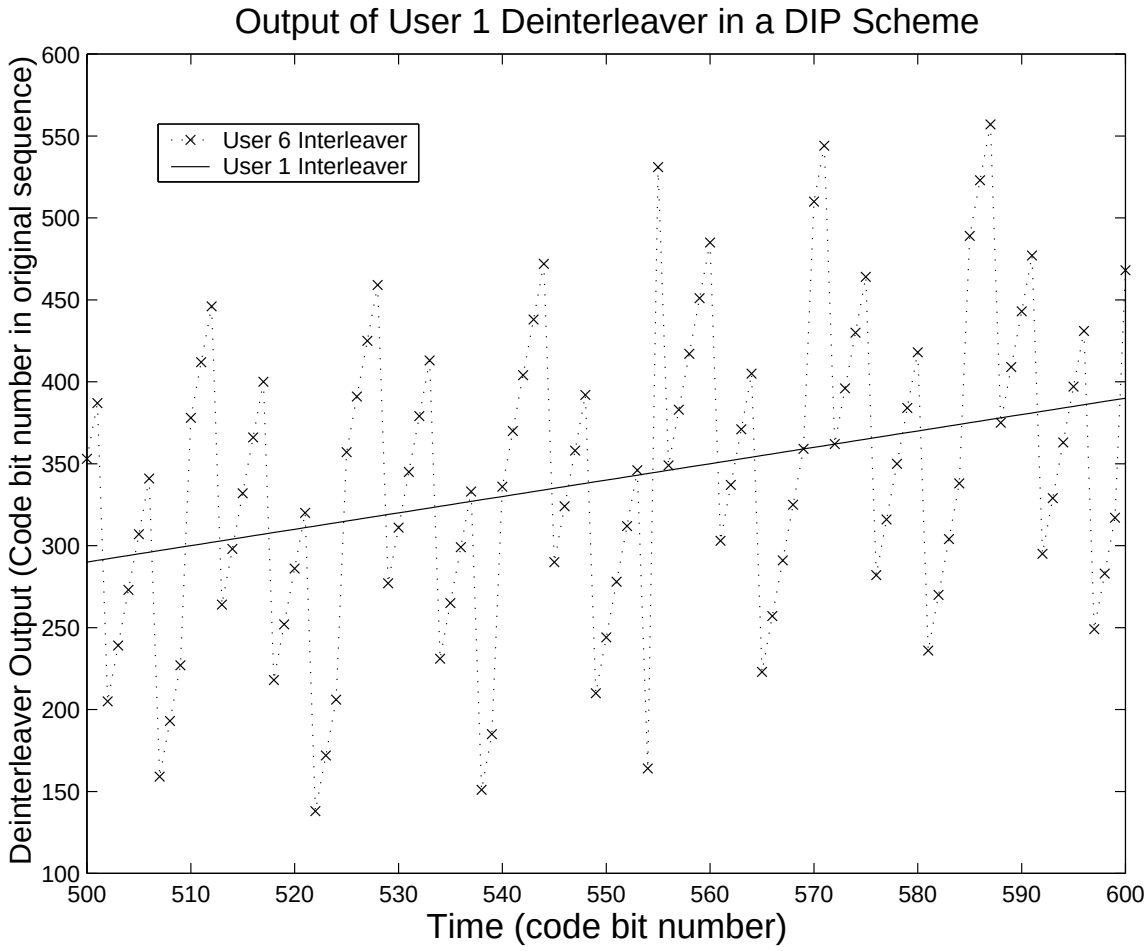

Figure 5: The output of User 1 Deinterleaver for a sequence interleaved by Pattern 6.

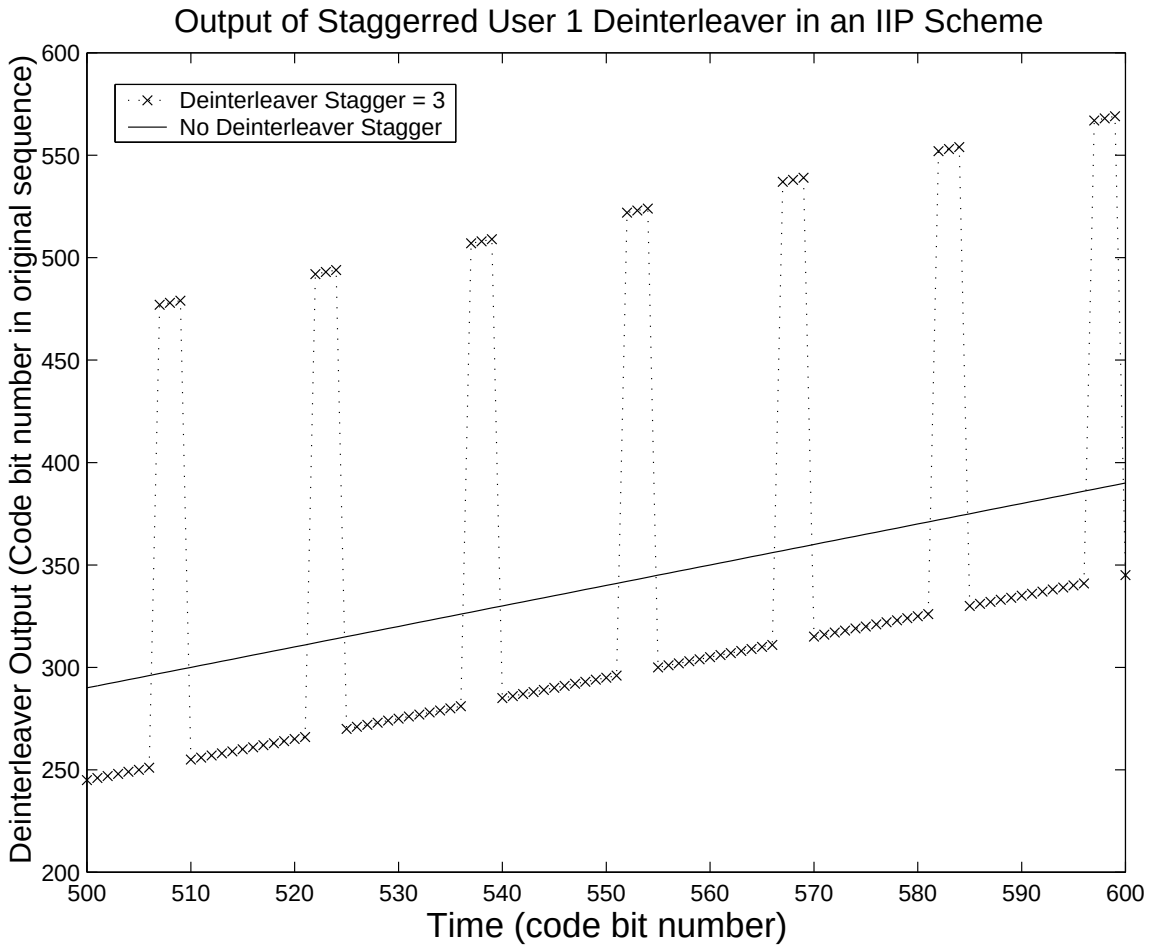

Figure 6: The output of User 1 Deinterleaver in an IIP scheme for a sequence deinterleaved with a stagger.

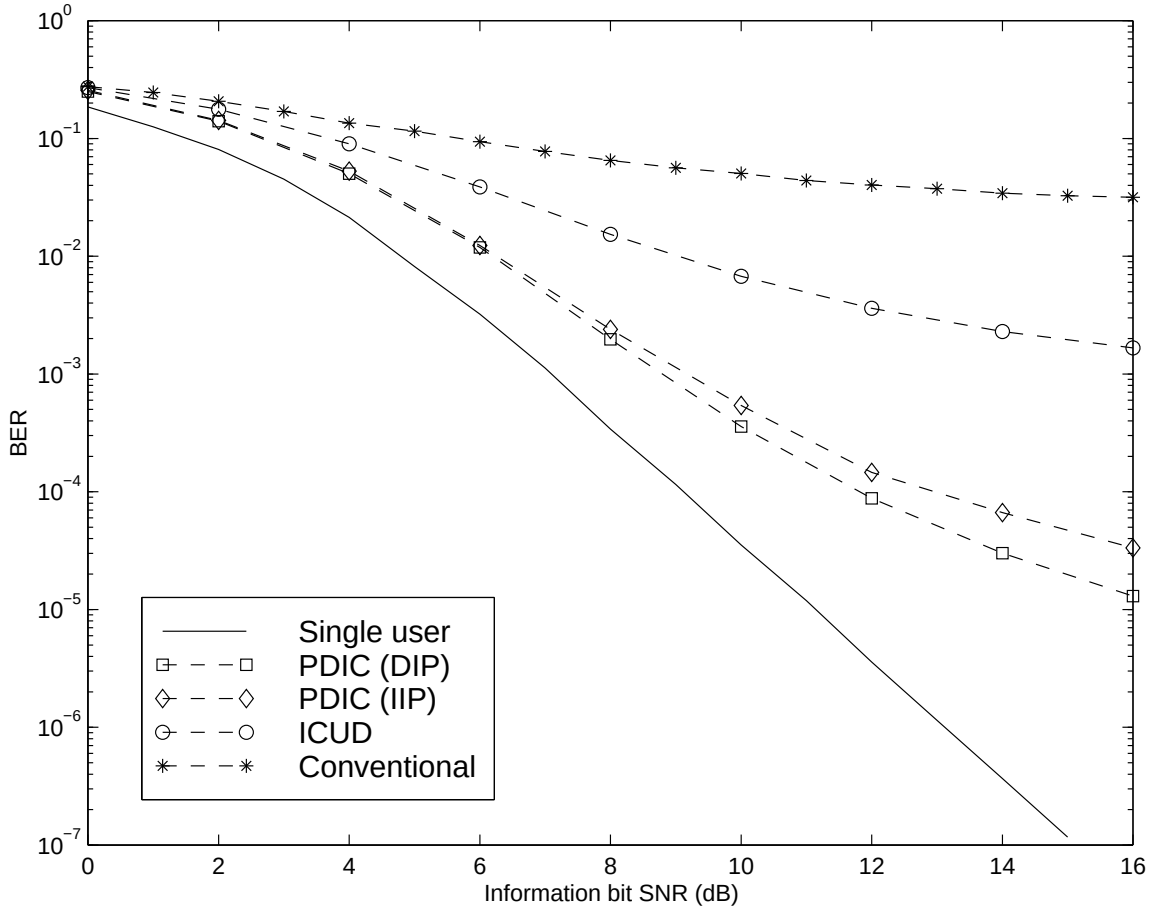

Figure 7: PDIC (DIP and IIP) versus ICUD for 8 users with $r = 0.35$ on the flat frequency-nonselective Rayleigh fading channel. The single-user bound and conventional detector performance are shown for reference.

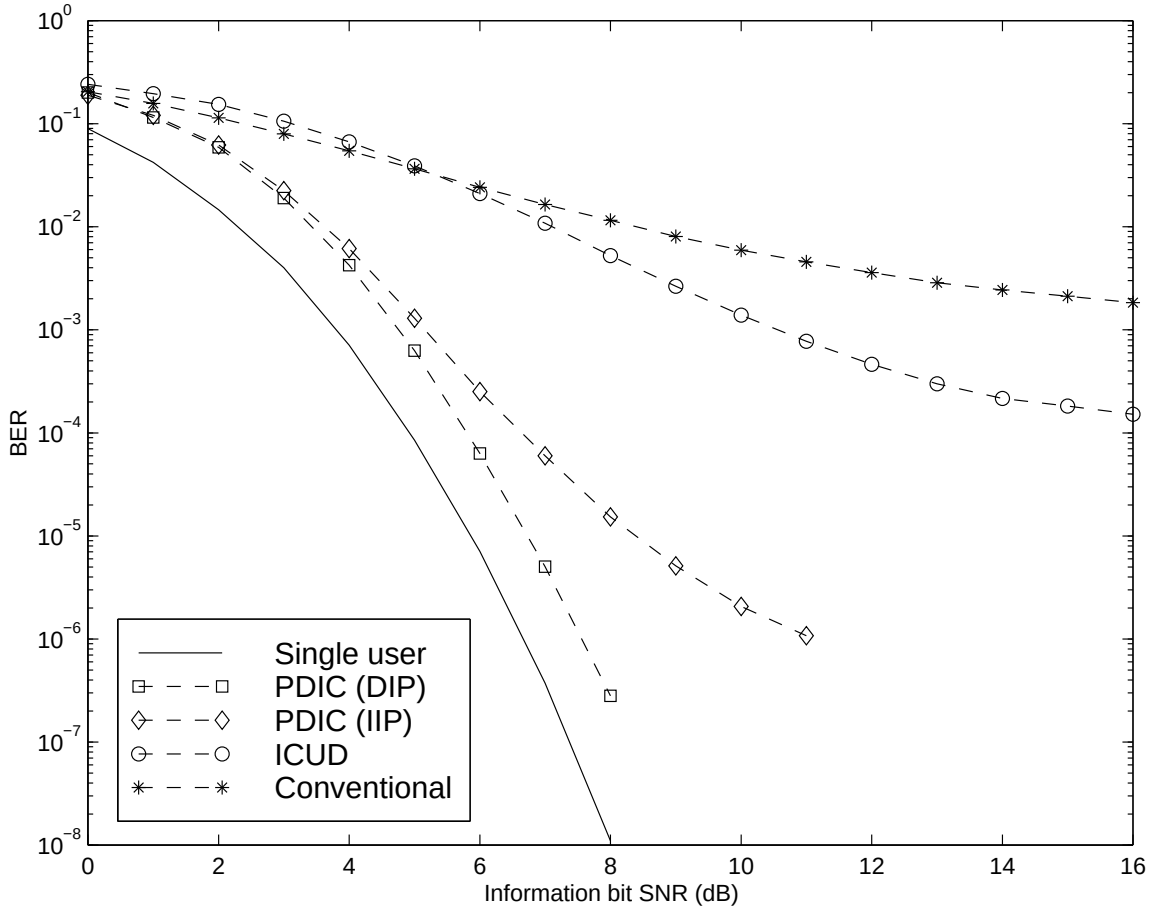

Figure 8: PDIC (DIP and IIP) versus ICUD for 8 users with $r = 0.25$ on the AWGN channel. The single-user bound and conventional detector performance are shown for reference.

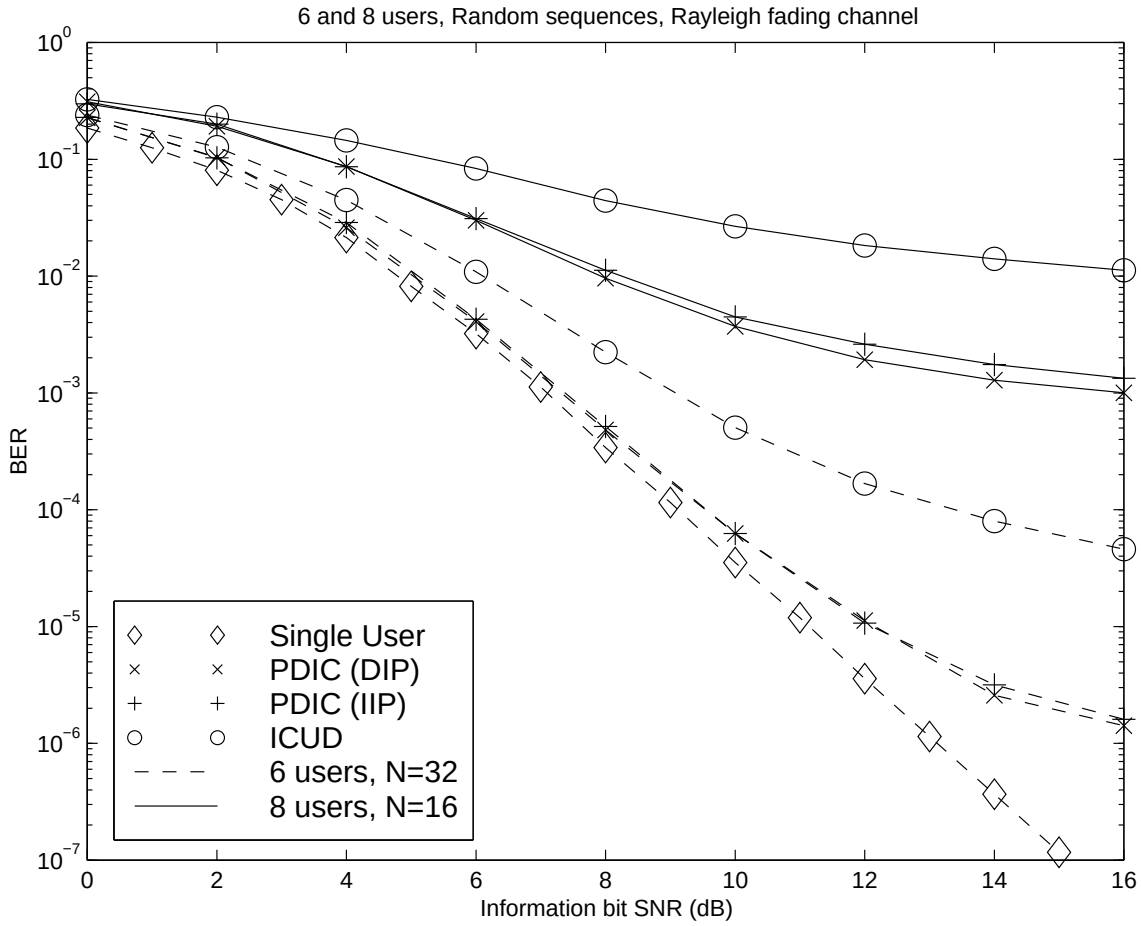

Figure 9: PDIC, with and without DIP, versus ICUD for 6 users with $\grave{N} = 32$ and 8 users with $\grave{N} = 16$ on the flat frequency-nonselective Rayleigh fading channel. In the legend, N represents $\grave{N}$.

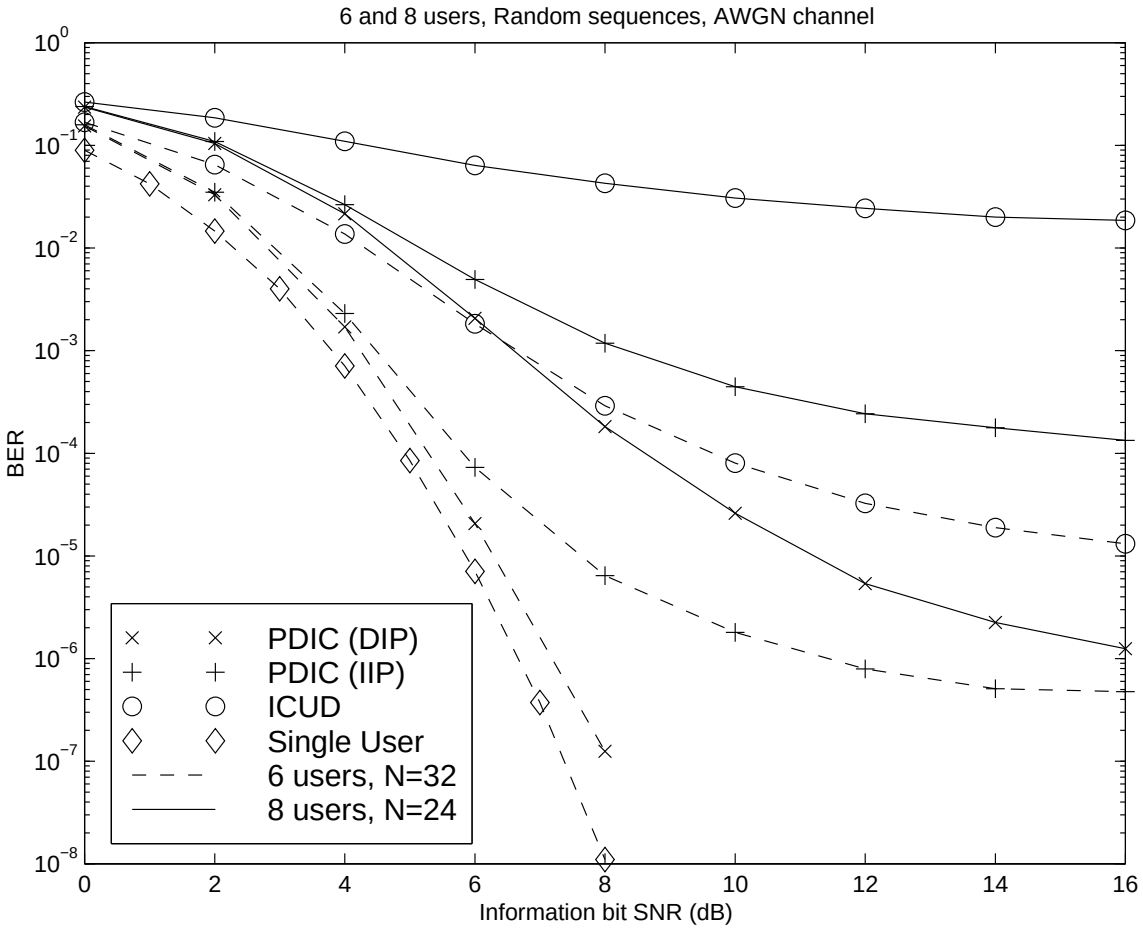

Figure 10: PDIC, with and without DIP, versus ICUD for 6 users with $\grave{N} = 32$ and 8 users with $\grave{N} = 24$ on the AWGN channel. In the legend, N represents $\grave{N}$.

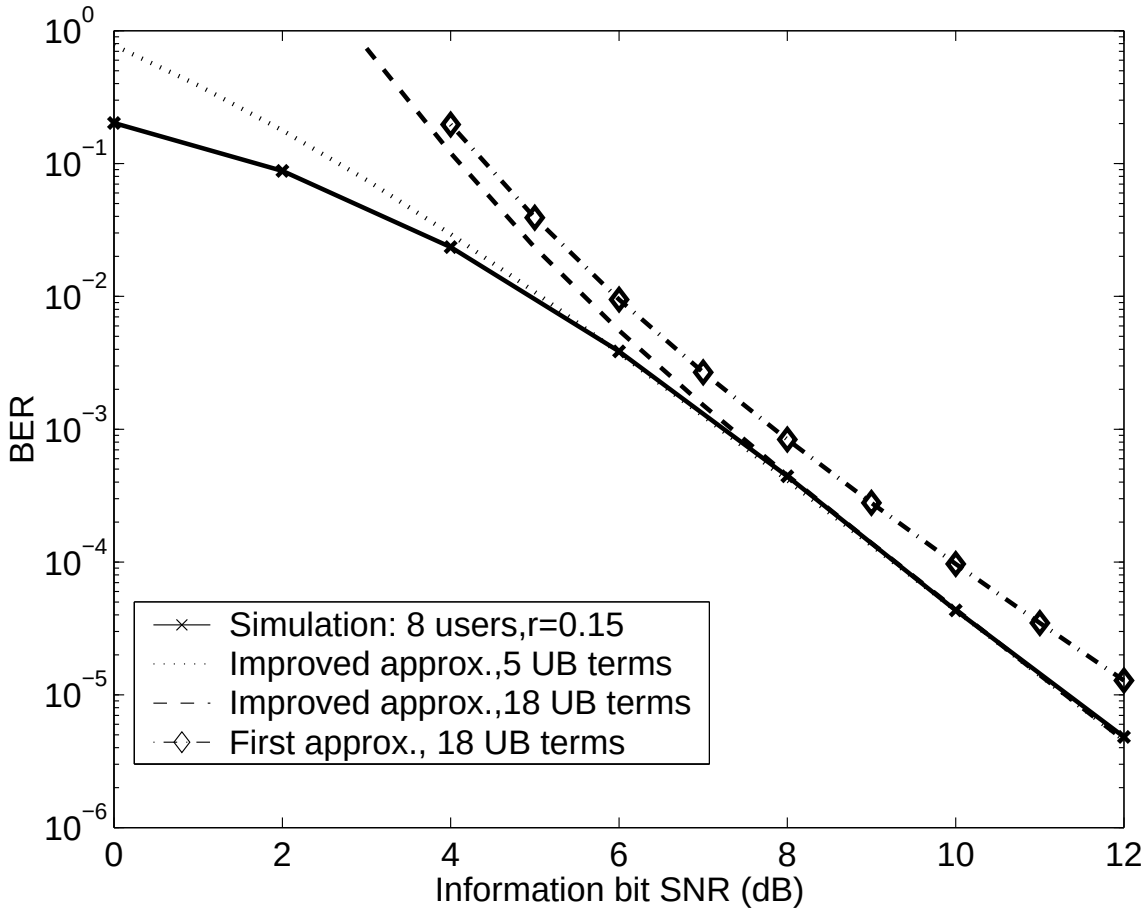

Figure 11: Approximate versus simulated BER of the ICUD scheme for an 8-user system with $r = 0.15$ on the fading channel.

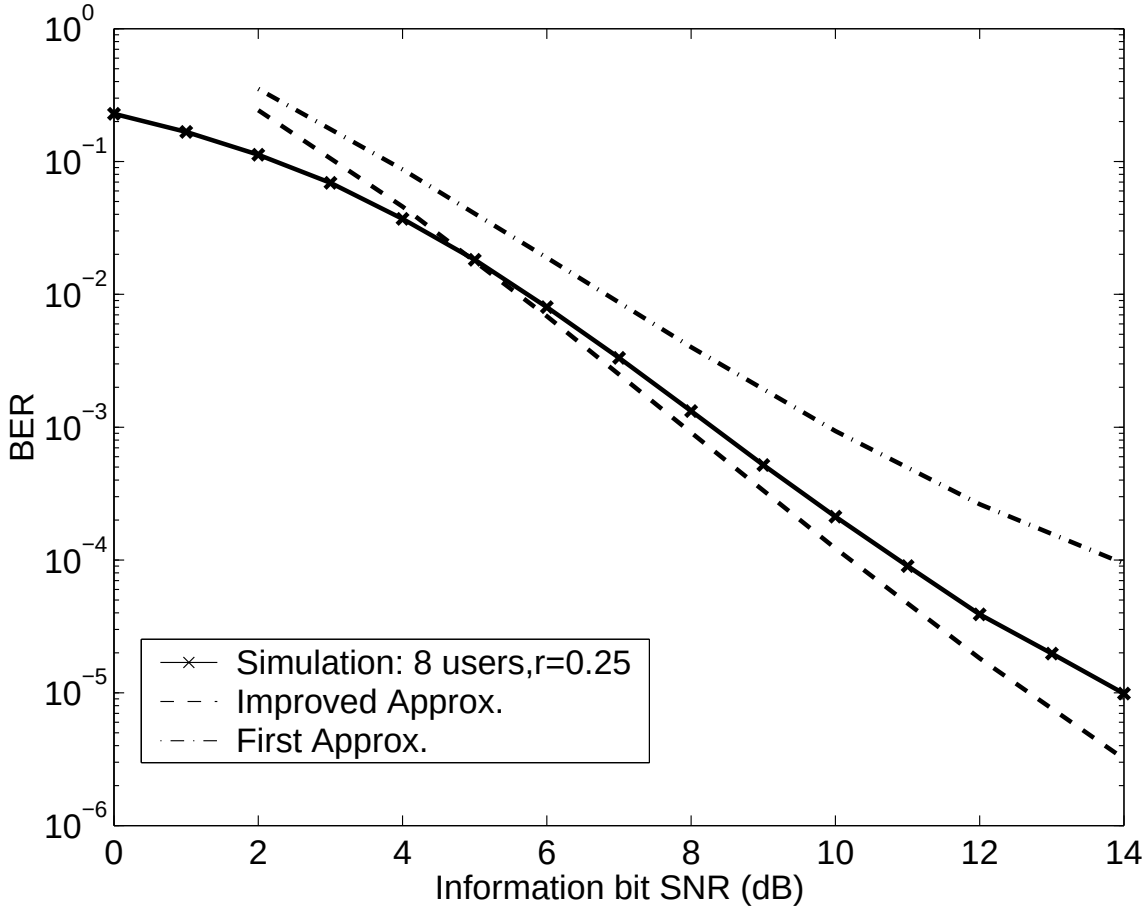

Figure 12: Approximate versus simulated BER of the ICUD scheme for an 8-user system with $r = 0.25$ on the fading channel. 5 UB terms used.

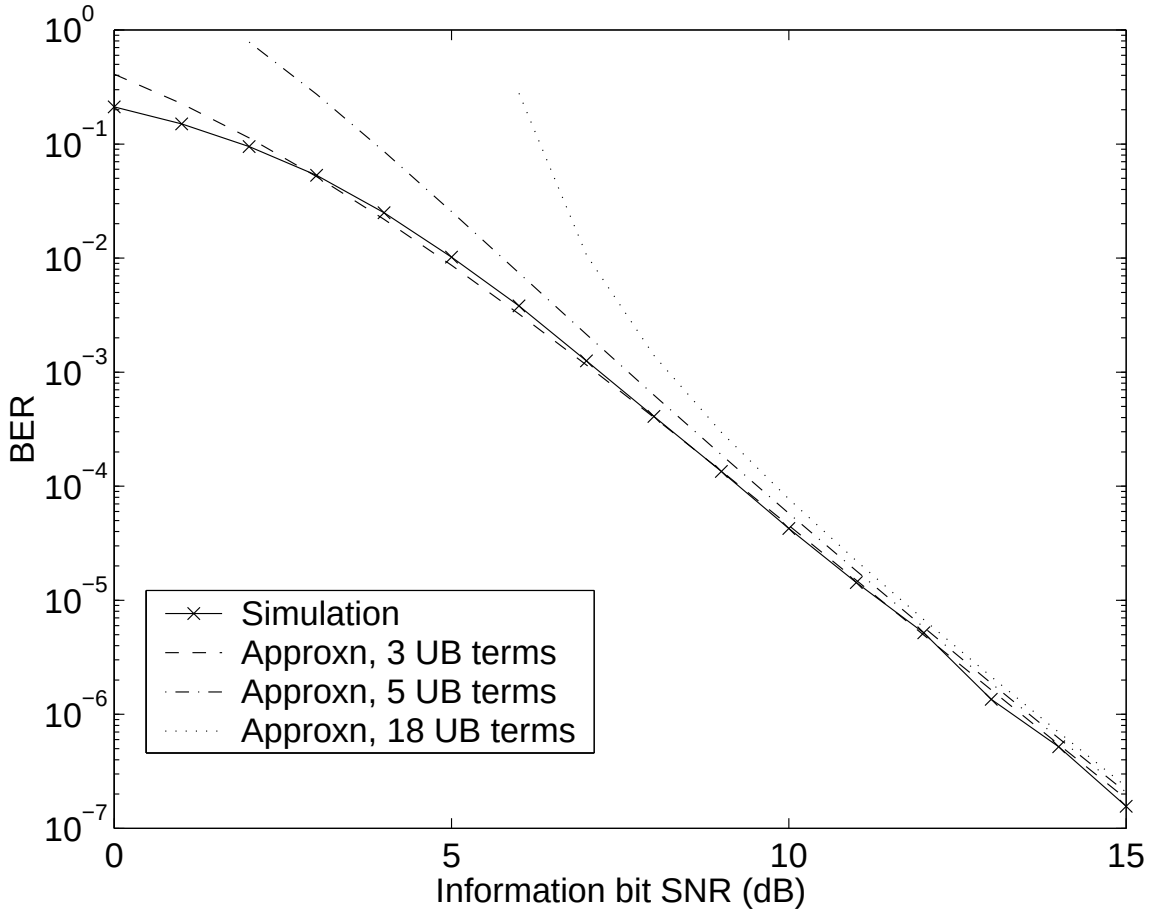

Figure 13: Approximate and measured BER for 8 users with $r = 0.25$ using PDIC with DIP on the Rayleigh fading channel.